Ancient Carbonate Tidalites

21

Yaghoob Lasemi, Davood Jahani,
Hadi Amin-Rasouli, and Zakaria Lasemi

Abstract

Carbonate tidalites are sediments deposited in supratidal, intertidal and the adjacent shallow subtidal environments by tidal, biogenic, chemical and diagenetic processes and are among the most common deposits in ancient carbonate platform successions. This chapter illustrates sedimentary facies, environments of deposition, and stratigraphy of carbonate tidalites and describes a few analogs from ancient deposits that commonly are encountered in the geological record. Ancient carbonate tidalites consist of a variety of constituents and diagnostic features formed during deposition and early diagenesis in different environments of a tidal system. Peritidal facies are arranged into meter-scale, commonly shallowing-upward succession of subtidal- to tidal flat facies known as parasequence, and may constitute the bulk of the transgressive and highstand packages of a depositional sequence. The geological record of ancient carbonate tidalites indicates deposition in the proximal areas of a tropical sea, particularly during global relative sea level highstands, in carbonate platforms and environments that have recurred many times since the Paleoproterozoic.

Y. Lasemi (✉) • Z. Lasemi
Illinois State Geological Survey, Prairie Research Institute, University of Illinois at Urbana-Champaign, Champaign, IL 61820, USA
e-mail: ylasemi@illinois.edu; zlasemi@illinois.edu

D. Jahani
Department of Geology, Faculty of Basic Sciences, North Tehran Branch, Islamic Azad University, Tehran, Iran
e-mail: d_jahani@iau-tnb.ac.ir

H. Amin-Rasouli
Department of Geosciences, University of Kurdistan, Sanandaj, Iran
e-mail: H.Aminrasouli@uok.ac.ir

21.1 Introduction

Tidalites are sediments deposited by tidal currents and are characterized by a distinct combination of sedimentary structures, textures, lithologies, and vertical successions reflecting various phases of tidal sediment transport in carbonate and siliciclastic tidal flat and shallow subtidal environments (Klein 1971, 1998). The term tidalites is somewhat synonymous with peritidal sediments, sediments formed near the tidal zone (Wright 1984; Flügel 2010; Pratt 2010), which

R.A. Davis, Jr. and R.W. Dalrymple (eds.), *Principles of Tidal Sedimentology*,
DOI 10.1007/978-94-007-0123-6_21, © Springer Science+Business Media B.V. 2012

designate deposits of a tidal flat system comprising supratidal, intertidal, and the adjacent shallow subtidal environments. Carbonate tidalites, formed as a result of tidal, biogenic, chemical and diagenetic processes, are among the most common deposits in ancient tropical carbonate platform successions. They have been deposited under arid or humid conditions in carbonate platforms (Read 1985; Pomar 2001) associated with a variety of sedimentary basins. This chapter first summarizes the diagnostic features and characterizes sedimentary facies, environments of deposition, and stratigraphy of ancient carbonate tidalites. This will be followed by a few illustrative examples of ancient carbonate tidalites related to passive margins, intracratonic, failed rift, and foreland basins.

Our understanding of the deposition and early diagenesis of carbonate tidal deposits grew significantly during the 1960s and 1970s as a result of comprehensive studies of many modern shallow and marginal marine carbonate environments (reviews in Bathurst 1975; Tucker and Wright 1990; Flügel 2010) that included studies in the Persian Gulf (e.g. Purser 1973), the Bahamas (e.g. Hardie 1977), south Florida (e.g. Enos and Perkins 1977) and western Australia (e.g. Logan et al. 1970). The application of these results and observations obtained from modern siliciclastic tidal flat environments (e.g. Reineck 1972) to ancient carbonate deposits (e.g. Ginsburg 1975; Hardie and Shinn 1986; Carozzi 1989), using Walther's Law (Middleton 1973) and the comparative sedimentology approach of Ginsburg (1974), led to accurate interpretations of facies, depositional environments and sequences of carbonate tidal deposits in the sedimentary record. Carbonate tidalites encompass a wide variety of characteristic depositional and diagenetic features analogous to their modern counterparts (e.g., Grotzinger 1989; Demicco and Hardie 1994, Flügel 2010). These features record important information on water level and tidal range, depth and energy level, salinity, climate and sea level history during deposition.

21.2 Tidal Processes

Tide is a periodic fluctuation in water level in a marine realm that is created by the gravitational pull of the moon and sun (Davis 1983; Dalrymple 1992) with the moon, being closer to earth, exerting the most gravitational force. In a tidal cycle, rising water generates the landward flood tidal current, but the fall generates the seaward and normally weaker ebb tidal current. A tidal cycle normally occurs twice daily (semidiurnal), but once a day (diurnal) or mixed diurnal and semidiurnal cycles may occur depending on tidal regime or local conditions (Davis 1983). The height of the water column between normal high tide and low tide levels is known as tidal range. During new and full moon, alignment of the moon, sun and earth generates a greater than normal tidal range (spring tide); conversely, during first and third quarters of a lunar cycle, a minimal tidal range (neap tide) occurs (Davis 1983). Based on variation of tidal range, shorelines are classified into macrotidal (>4 m), mesotidal (2–4 m) and microtidal (<2 m). In macrotidal areas, tide dominates over other processes and most mesotidal and microtidal areas are wave and storm dominated, but tide domination may even occur in a protected microtidal coast where wave action is limited (Dalrymple 1992). In contrast to their siliciclastic counterparts, most modern peritidal carbonate environments are microtidal (Wright 1984; Pratt et al. 1992).

21.3 Depositional Environments

The daily fluctuation of water level subdivides the tidal system into three bathymetric belts including subtidal (below mean low tide level), intertidal and supratidal environments (Fig. 21.1a) that are characterized by a set of biological, physical and chemical processes. The subtidal environment may extend for hundreds of kilometers offshore depending on tectonic and geographic settings. It is the major source of sediment for the adjacent tidal flat setting and comprises low energy back barrier lagoons of various salinity and areal extent, platform margin (carbonate barriers/sand shoals) and open marine environments (Fig. 21.1). The intertidal environment lies between mean low tide and mean high tide levels (Fig. 21.1a) and is exposed once or twice daily during each tidal cycle. This zone in part includes isolated ponds and meandering tidal channels that are essentially subtidal environments occurring within the intertidal belt (Fig. 21.2). The supratidal environment lies above the mean high tide level (Fig. 21.1a) and is flooded only during spring tides (twice each month) and less frequent storm tides. It is widespread in mainland coasts, but narrow supratidal environment develops on channel levees and beach ridges within the intertidal belt (Fig. 21.2b). In an arid climate, the supratidal environment is evaporitic and is

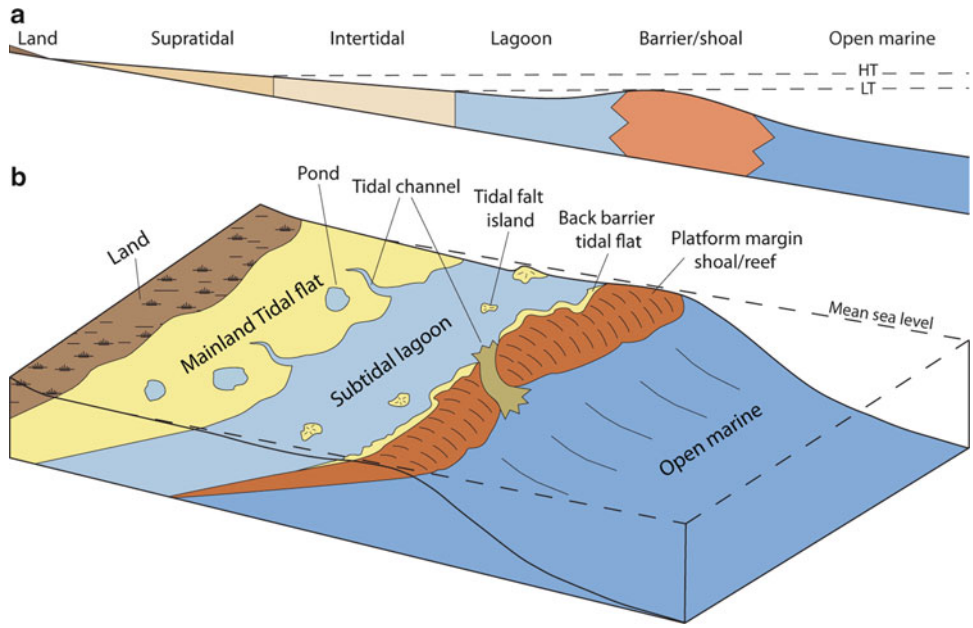

Fig. 21.1 Carbonate platform paleogeography and various depositional environments of a tidal system. (**a**) A gently sloping carbonate ramp profile showing depositional environments and their relationship to sea level (**b**) Block diagram of a carbonate shelf showing various areas of tidal flat development. Note that platform margin barrier/shoal and tidal flat environments are dissected by tidal channels. Abbreviations: *HT* high tide, *LT* low tide

known as "sabkha" (Fig. 21.2a) named after the evaporitic supratidal flats of the southern part of the Persian Gulf. In humid climate, supratidal flat is characterized by an extensive freshwater marsh (Fig. 21.2b).

Tidal flats normally develop in shorelines protected from waves and fluvial-deltaic influence and are the most extensive in mainland coasts, but narrower tidal flats occur in the back of islands or carbonate barriers/shoals at the platform margin (Fig. 21.1b). In ancient carbonate platforms, the back barrier tidal flats could have been quite extensive (see the Precambrian tidalites in Sect. 21.7.1). Ancient carbonate tidal flats could have also developed on low-relief supratidal islands and intertidal banks surrounded by subtidal environment (Pratt and James 1986; Pratt 2010). On a windward-facing tidal flat, beach ridges at the seaward edge of intertidal flat (Fig. 21.2b) or distinct barrier islands separated from the intertidal flats by a subtidal lagoon of variable width (Fig. 21.2a), analogous to siliciclastic barrier islands, may develop (Shinn 1986). In unprotected coasts exposed to high energy waves, such as the eastern and western parts of the Persian Gulf Abu Dhabi Embayment and the windward northern side of the Persian Gulf barrier islands (Purser and Evans 1973), tidal flats are not well developed. In these coasts, the shoreline is covered by high energy beach environment. In cool-water settings, too, tidal flats are scarce and the shoreline deposits are characterized by high energy sand- to gravel-size carbonate beach facies commonly backed by carbonate aeolianites (James 1997).

21.4 Processes of Sedimentation

Carbonate sediments form *in situ*, mainly by carbonate secreting organisms in the subtidal environments (e.g. Wilson 1975; Flügel 2010); part of the subtidal carbonate sediment is transported landward by storms and tidal currents and deposited in the intertidal and supratidal environments of the tidal flat system. In the subtidal lagoon, current energy and grain size normally decreases seaward toward the deeper outer shelf-lagoon. In this setting, quiet water condition results in accumulation of lime mud of biological (e.g. Robbins and Blackwelder 1992; Pratt 2001) and possibly chemical origin (Shinn et al. 1989), which may be stabilized by sessile organisms, such as seagrass and calcareous algae. In the subtidal and adjacent intertidal settings, bioturbation by burrowing organisms (except for extreme conditions, such as hypersalinity

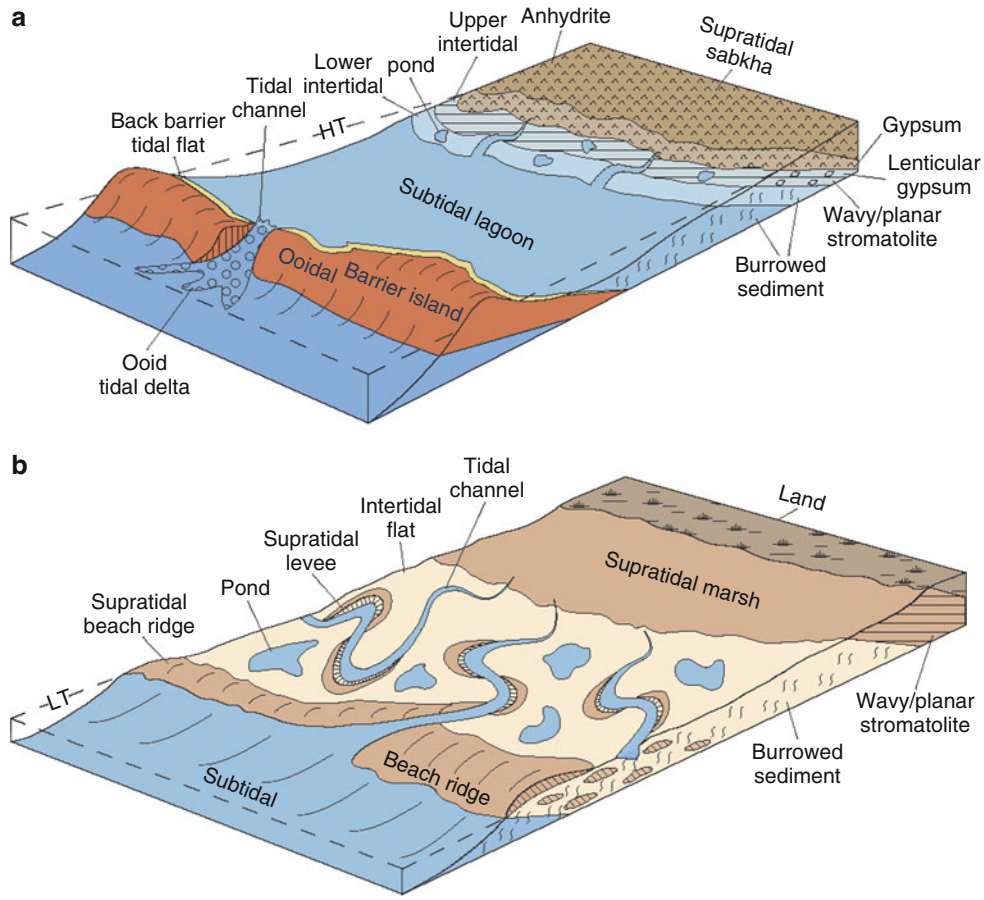

Fig. 21.2 Diagrams showing major depositional settings of modern arid (Persian Gulf) and humid (Bahamas) tidal systems (Modified from Shinn 1983a). (**a**) Major subtidal and tidal flat facies and sedimentary environments of the southern Persian Gulf inner ramp setting. An ooidal barrier island separates the open sea from the quiet back barrier subtidal lagoon. Note the development of ebb ooid tidal delta and a narrow tidal flat in the back of the barrier island. Note also the presence of bioturbated sediment in the lower intertidal, lenticular gypsum bearing planar/wavy stromatolite in the upper intertidal and gypsum/anhydrite deposits in the supratidal zone. (**b**) Major facies and environments of the Andros Island tidal flat system. Supratidal zones are shown in *light brown*. Note the burrowed deposits in the intertidal and planar/wavy stromatolite in the supratidal freshwater marsh environments, respectively. Note also the presence of beach ridge at the seaward edge of intertidal zone, and the supratidal areas on the beach ridge and tidal channel levees. Abbreviations: *HT* high tide, *LT* low tide

or strong current energy) may destroy primary fabrics and structures of sediments; intensity of bioturbation and skeletal diversity decrease with increasing salinity. In various environments of a tidal flat system, current energy and grain size decreases in a landward direction and various processes, such as desiccation, cementation and dolomitization operate. In various environments of a tidal system, binding and trapping of sediment and carbonate precipitation by bacteria and cyanobacteria lead to microbial deposits (see the following section). In the tidal flat setting, evaporation results in higher salinity leading to cementation and primary micritic dolomite formation. Early cementation prevents compaction of soft and muddy sediments, leading to preservation of peloids, intraclasts and primary sedimentary fabrics and structures.

The high energy conditions of the platform margin result in the development of barrier reefs and/or carbonate sand shoals, which separate the often restricted back-barrier environments from the open sea. As a result of tidal current activity, the margin is normally dissected by tidal channels that connect the open-ocean water with that of the quiet back-barrier subtidal environment. Depending on tidal regime, the mouths of these channels may develop tidal deltas. In the Abu Dhabi region of southern Persian Gulf, for example,

ebb ooid tidal deltas are developed seaward of tidal channels (Fig. 21.2a) that cut through the wave-formed oolitic barrier island complex (Purser and Evans 1973).

21.5 Facies Belts and Their Diagnostic Features

Periodic changes in the direction and speed of tidal currents, differences in environmental conditions within the inner shelf, biogenic activity of organisms, and intermittent exposure of the proximal areas of a tropical carbonate platform result in various facies in different environments of a tidal system. These facies are characterized by a variety of constituents and diagnostic features formed during deposition and early diagenesis. Tidal flat deposits commonly consist of thin bedded and laminated lime mudstones/dolomudstones or microbial laminae known as laminites (Fig. 21.3a–c). They are tan to light brownish gray in the field as opposed to gray-colored subtidal facies formed under a relatively reducing condition (Fig. 21.3d). Some tidal flat deposits consist of mixed carbonate and clay- to sand-sized siliciclastics indicating proximity to aeolian or fluvial/deltaic systems or intermittent advance of siliciclastics from a nearby upland area during floods (see the Middle Cambrian tidalites in Sect. 21.7.2). Tidal flat and subtidal facies are interlayered with various erosive-based, graded intraclastic storm deposits ("tempestites") in some stratigraphic intervals (e.g., Wignall and Twitchett 1999, Y. Lasemi et al. 2008) recording deposition in a storm dominated platform (see the Middle Cambrian and the Lower Triassic tidalites in Sects. 21.7.2 and 21.7.5.1). Carbonate storm beds commonly consist of intraclasts (edgewise conglomerate) of various facies (Fig. 21.4a, b) and/or ooids, peloids and bioclasts of mixed fauna and normally display hummocky cross-stratification, lamination, and gutter casts (Fig. 21.4c, d). Repeated storm events may partially or completely remove the previously deposited tidal sediments leading to stacked storm deposits (Fig. 21.4 c, d).

21.5.1 Subtidal Belt

The quiet water, back-barrier lagoon facies generally are muddy and consist of characteristic gray and bioturbated mudstone to packstone texture (Figs. 21.3d and 21.5a, b). These sediments generally contain microbial pisoids known as oncoids (see below), peloids, low diversity skeletal components including gastropods, ostracods, green algae, and benthic foraminifera or abundant numbers of a certain individual biota depending on climate and salinity (Fig. 21.5c, d). Open marine and restricted subtidal lagoon sediments may comprise microbial structures known as microbialites.

Microbialites are organosedimentary deposits formed by interactions between biological, environmental and diagenetic processes as a result of benthic microbial organisms that trap and bind sediment and/or form the locus of calcium carbonate precipitation (Burne and Moore 1987). Trapping and binding mechanisms and early diagenetic calcification and/or precipitation by bacteria appear to be the major processes for the formation and preservation of microbialites in modern marine subtidal and tidal flat environments (e.g., Riding 2000; Reid et al. 2000; Dupraz et al. 2009). Marine microbialites include the non-laminated structures with macroscopic, dark-colored clotted fabric (Fig. 21.6a) referred to as thrombolites and laminated forms (Fig. 21.6b, f) known as stromatolites (e.g., Pratt and James 1982; Riding 1999, 2000) commonly constructed by filamentous calcified (Fig. 21.6c) and non-calcified (Fig. 21.6d, f) bacteria. Microbialites represent arid upper intertidal (Fig. 21.2a), humid supratidal marsh (Fig. 21.2b), hypersaline subtidal- to intertidal and normal marine platform margin environments.

Stromatolite pisoidal (Figs. 21.5d and 21.6c, d) and columnar microbialite structures (Fig. 21.6b, e) forms represent both modern and ancient open marine and restricted subtidal sediments as old as 3.5 Ga (e.g. Grotzinger 1989; Riding 2000), but thrombolites are normally found in Phanerozoic subtidal deposits. Sediment of a high energy restricted lagoon may contain columnar stromatolite and ooids/skeletal grains derived from the nearby platform margin (see The Precambrian and Middle Cambrian tidalites in Sects. 21.7.1 and 21.7.2). Laterally extensive interlayered gypsum/anhydrite-bearing dolomudstone/limestone and layered nodular anhydrite with no evidence of subaerial exposure (Fig. 21.7) may record deposition in a subtidal lagoon environment where the water became increasingly saline due to poor circulation.

The upper subtidal sediment in high energy exposed coasts typically consists of beach facies characterized by flat-laminated to cross-bedded grainstone facies. These strata may contain skeletal grains and/or ooids,

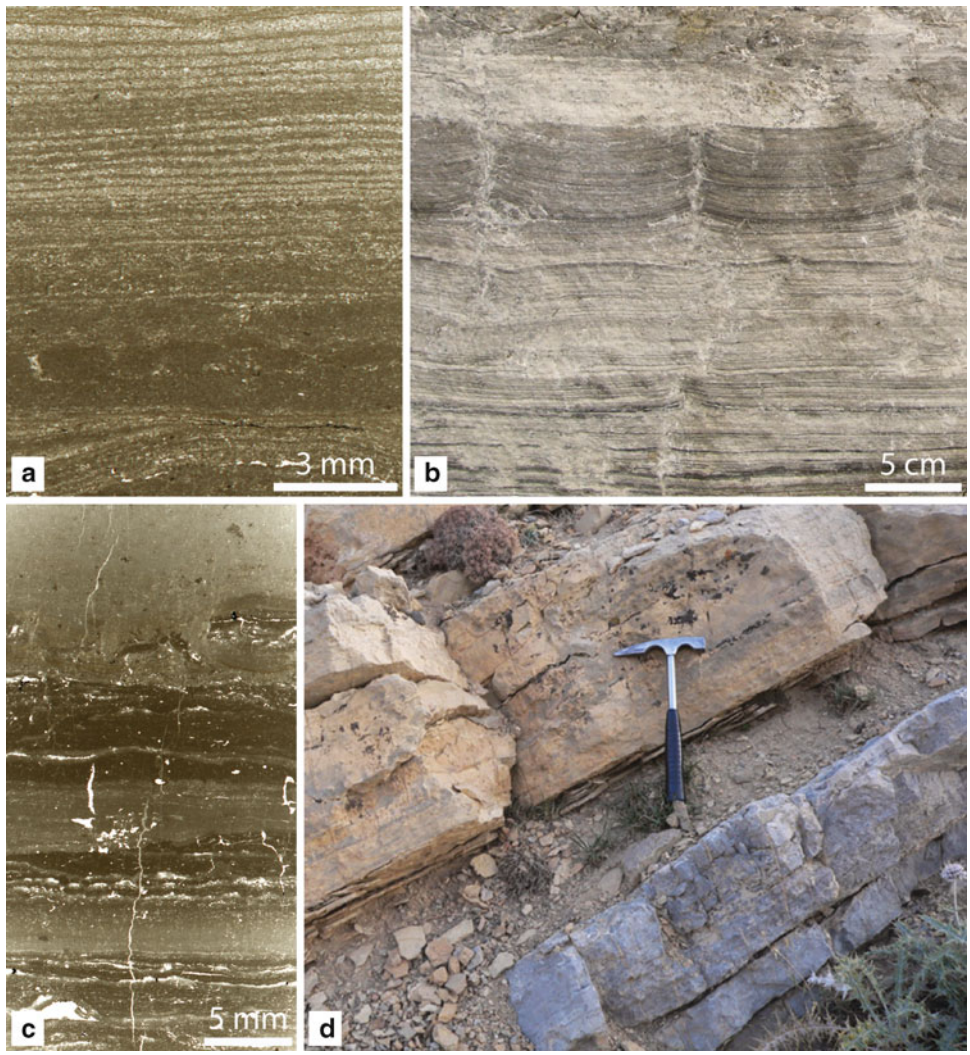

Fig. 21.3 (**a**–**c**) Laminated tidal flat deposits and (**d**) intertidal and lagoonal deposits: (**a**) Thin section photograph showing interlamination of mud and fine sand- to silt-size carbonate. Note cement-filled desiccation crack in the *lower left*. Thickness variation of the laminae may reflect daily variation of tidal range (neap-spring cycles); Cave Hill Member of the Mississippian Kinkaid Formation in the Buncombe Quarry, southern Illinois. (**b**) Mud-cracked laminated tidal flat facies in the Middle Devonian Vernon Fork Member of the Jeffersonville Limestone, southwest Indiana (Photo courtesy of Dr. B.D. Keith, Indiana geological Survey). (**c**) Thin section photograph of interlaminated planar- to wavy stromatolite (*darker laminae*) and dolomudstone. The graded intraclastic upper lamina was formed by a storm tide; Cave Hill Member of the Mississippian Kinkaid Formation in the Kinkaid Creek section, southern Illinois. (**d**) Field photograph of a succession composed of *bluish gray* subtidal limestone overlain by *light grayish brown* to tan intertidal dolomudstone. The contact between the subtidal and intertidal facies appears to be sharp; Lower Triassic lower member of the Elika Formation, Alborz Mountains, northern Iran

peloids and intraclasts (Fig. 21.8a) and may grade landward into a narrow belt of lower energy intertidal (foreshore) facies. The tidal channel deposits at the platform margin may consist of laminated horizontal strata and/or cross-bedded (sometimes bidirectional) gravel- and sand-size intraclastic ooid/bioclast grainstones (Fig. 21.8b) and/or columnar microbialites.

21.5.2 Intertidal Belt

The intertidal belt is flooded and exposed once or twice daily and consists of various facies with diagnostic features. The arid upper intertidal sediment commonly consists of mud-cracked laminated facies deposited by tidal currents (Fig. 21.3a, b) and/or planar to wavy

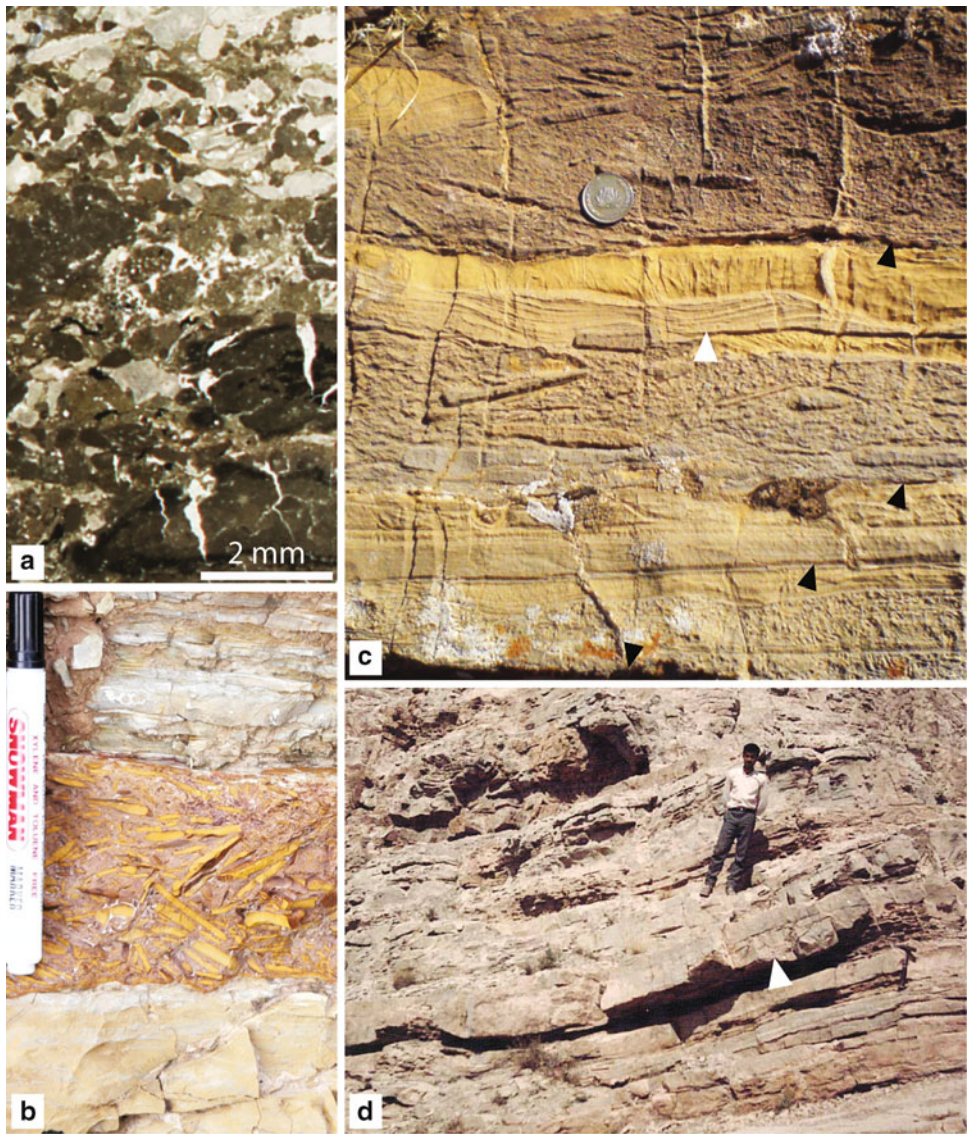

Fig. 21.4 Tidal flat storm deposits: (**a**) Photomicrograph of a thin section showing graded tidal flat storm bed composed of intraclasts (mainly mud-cracked stromatolite fragments), peloids and mixed fauna (the majority of the light grains are echinoderm debris); Cave Hill Member of the Mississippian Kinkaid Formation, Buncombe Quarry, southern Illinois. (**b**) Field photograph of a tidal flat succession intercalated by an erosive-based intraclast grainstone storm bed. The storm bed consists of yellow tidal flat dolomudstone; Lower Triassic lower member of the Elika Formation, central Alborz Mountains, northern Iran (magic marker is 14.5 cm long). (**c**) Stacked fining-upward erosive-based storm beds (*black arrows* at the basal erosional contacts) with intraclasts of subtidal/intertidal facies and hummocky cross-stratification (*white arrow*) (*coin* diameter is 2.5 cm). (**d**) *Reddish brown* very thin-bedded and laminated intertidal deposit intercalated by several erosive based intraclastic storm layers. Note the large gutter cast (*arrow*) that has cut through the underlying intertidal facies (above the hammer in the *lower right*) (Photo courtesy of Dr. M. Ghomashi, Sistan-Baluchistan University, Zahedan, Iran); Lower Triassic lower member of the Elika Formation, Bibishahrbano Mountain, northern Iran

stromatolite (Figs. 21.3c, 21.6f and 21.9d) (see the Triassic tidalites in Sect. 21.7.5 for an example). The lower intertidal environment adjacent to a hypersaline subtidal setting may comprise domal stromatolite structure (Fig. 21.9a–c) changing to wavy and planar stromatolite in a landward direction (see the Precambrian and Middle Cambrian tidalites in Sects. 21.7.1 and 21.7.2, respectively). Other features common in arid

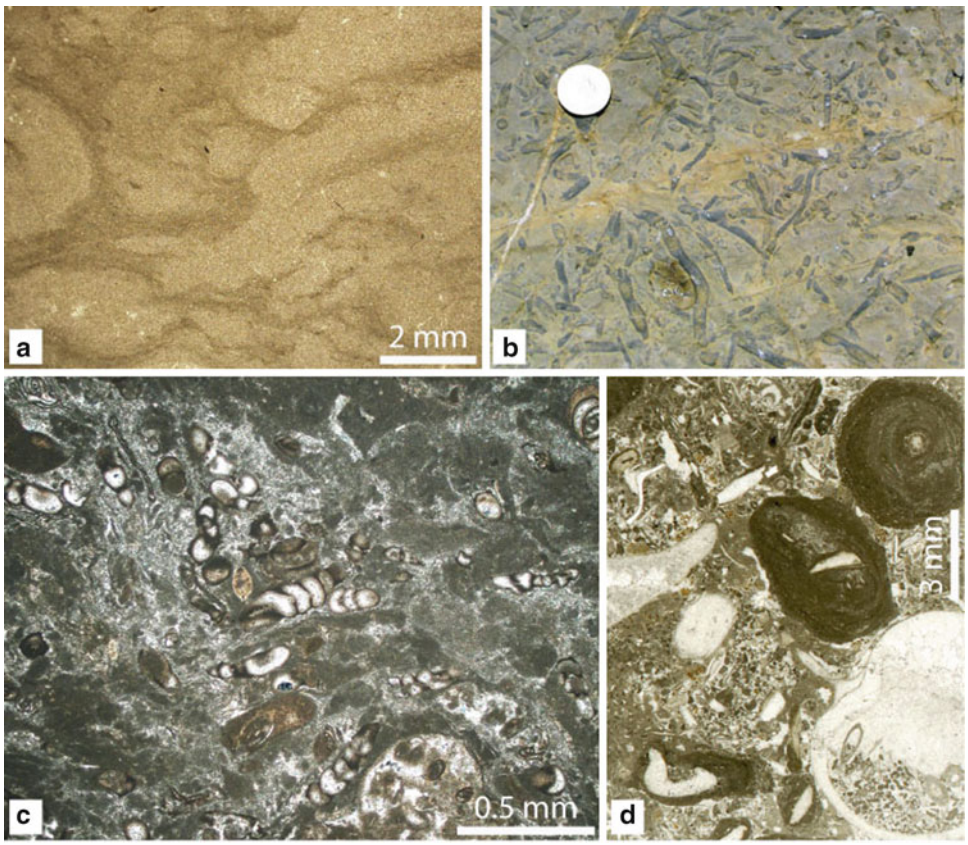

Fig. 21.5 Subtidal lagoon facies: (**a**–**b**) Heavily bioturbated lime mudstone subtidal facies in the Lower Triassic lower member of the Elika Formation of the Alborz Mountains, northern Iran. (**a**) Photomicrograph of a vertically oriented thin section showing abundant horizontal burrows in a lime mudstone (**b**) Upper surface of a heavily bioturbated subtidal lime mudstone bed (*coin* diameter is 2.5 cm). (**c**) Photomicrograph of a subtidal lagoon facies composed of peloids, intraclasts and restricted fauna (mainly dentritinid forams). Note a miliolid foram in the *upper right*; Lower Miocene Asmari Formation, Zagros Mountains, southwest Iran. (**d**) Thin section photograph of a peloidal bioclast oncoid packstone. Note the nearly concentric oncoids (pisoidal form of microbialites) in the *upper right*. Note also the geopetally filled gastropod shell mold in the *lower right* of the photograph; Negli Creek Member of the Mississippian Kinkaid Formation, southern Illinois

intertidal sediments include tepee structures (Fig. 21.10a–c) and gypsum crystals or their pseudomorphs (Figs. 21.9d and 21.10d, e).

Tepees as defined by Adams and Frenzel (1950) are structures having an inverted V-shaped profile similar to the American Indians tents. However, this form of tepee is only occasionally present and it normally appears as irregular and low ridges (Pratt 2002). Tepee structures (Fig. 21.10a–c) are common to peritidal deposits and form as a result of desiccation, cementation and crystal growth, thermal expansion, and contraction of partially lithified sediment in arid tidal flat or high energy shallow subtidal sediments (Kendall and Warren 1987). They reflect the polygonal antiform ridges arched along polygonal cracks in a cemented surface crust as seen in plan view (Demicco and Hardie 1994). In high energy subtidal settings, cementation of carbonate grainstone layers can lead to expansion and development of centimeter-scale to giant polygonal cracks that may be folded or thrusted at the margins forming tepee structures (e.g. Kendall and Warren 1987; Lokier and Steuber 2008). Tepees may also form as a result of brecciation of lithified sediment, regardless of their depositional setting, by syndepositional fault movement and subsequent cementation (Pratt 2002).

The lower intertidal sediment in high energy tide-dominated coasts, commonly consists of planar laminated and/or cross-bedded bioclast/peloid intraclast grainstone facies that grade landward to heterolithic

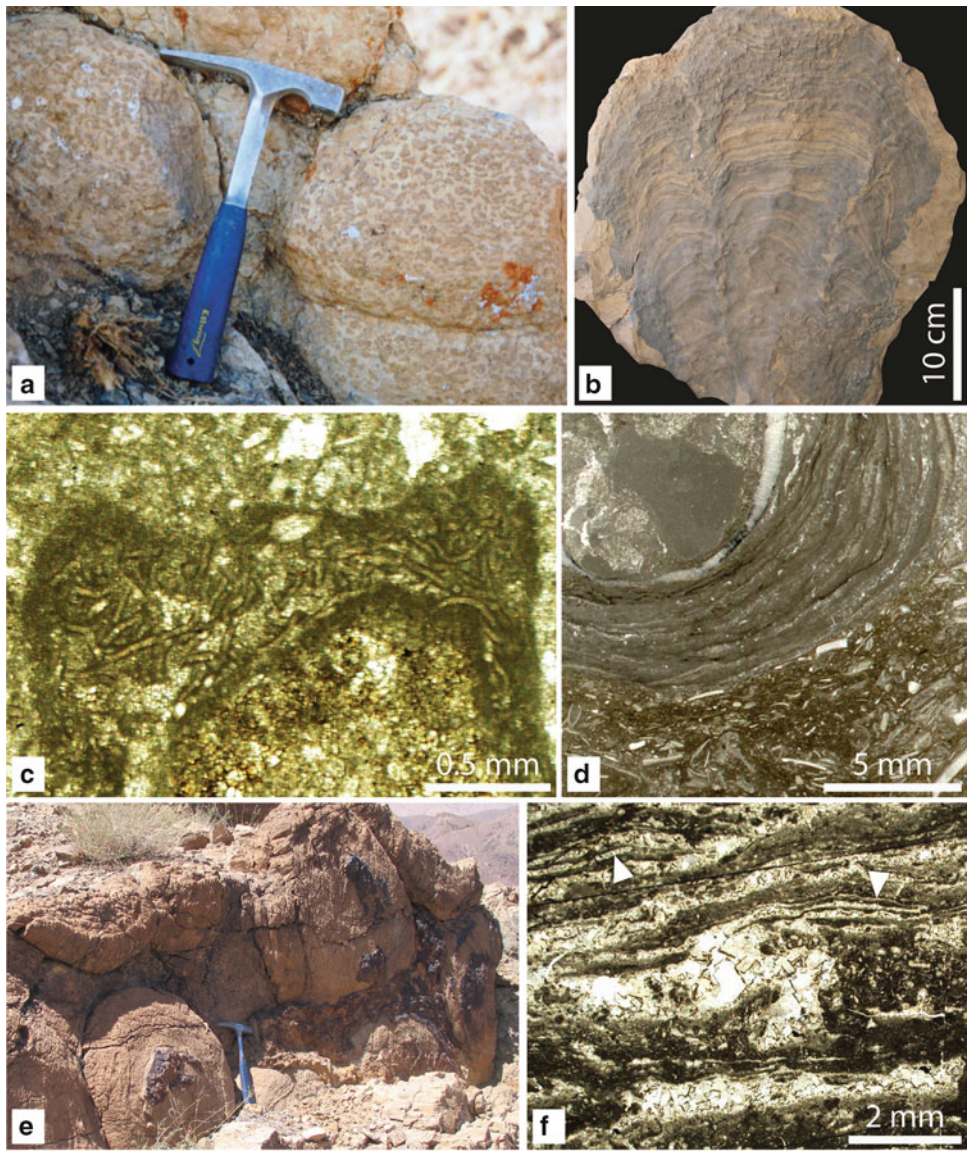

Fig. 21.6 Subtidal (**a** through **e**) and intertidal microbialites: (**a**) Shallow subtidal dome-shaped thrombolite structures with dark microbial clots and dolomite-field fenestral voids; Middle Cambrian member 1 of the Mila Formation, east central Alborz Mountains in northern Iran. (**b**) A branching columnar stromatolite from the Silurian deposits of the southern Tabas Basin, east central Iran. (**c**) Photomicrograph under normal light of a part of pisoidal form of stromatolite (*oncoid*) formed by calcified tubular cyanobacteria (*Girvanella*); Negli Creek Member, Mississippian Kinkaid Formation, east of Princeton, Kentucky. (**d**) Thin section photograph of a part of an oncoid in a peloidal bioclast oncoid packstone. The oncoid appears to have been formed by non-calcified cyanobacteria; Negli Creek Member, Mississippian Kinkaid Formation, southern Illinois. (**e**) A compound subtidal columnar stromatolite complex from the Middle Cambrian member 2 of the Mila Formation in central Alborz Mountains, northern Iran. (**f**) Photomicrograph of flat- to wavy-laminated stromatolite with cement-filled planar birdseyes (see Sect. 21.5.2) and molds of filamentous cyanobacteria (*arrows*); Middle Triassic middle member of the Elika Formation in the Alborz Mountains, northern Iran

layers of sand- to coarse silt-sized and mud-size sediments showing flaser to wavy and lenticular bedding. This millimeter- to centimeter-scale interlayering, referred to as rhythmites (Reineck and Singh 1980) and tidal bedding or heterolithic stratification (Demicco and Hardie 1994) form due to declining tidal current energy and the resulting change in sand to mud ratio in a landward direction, and represent deposition in the

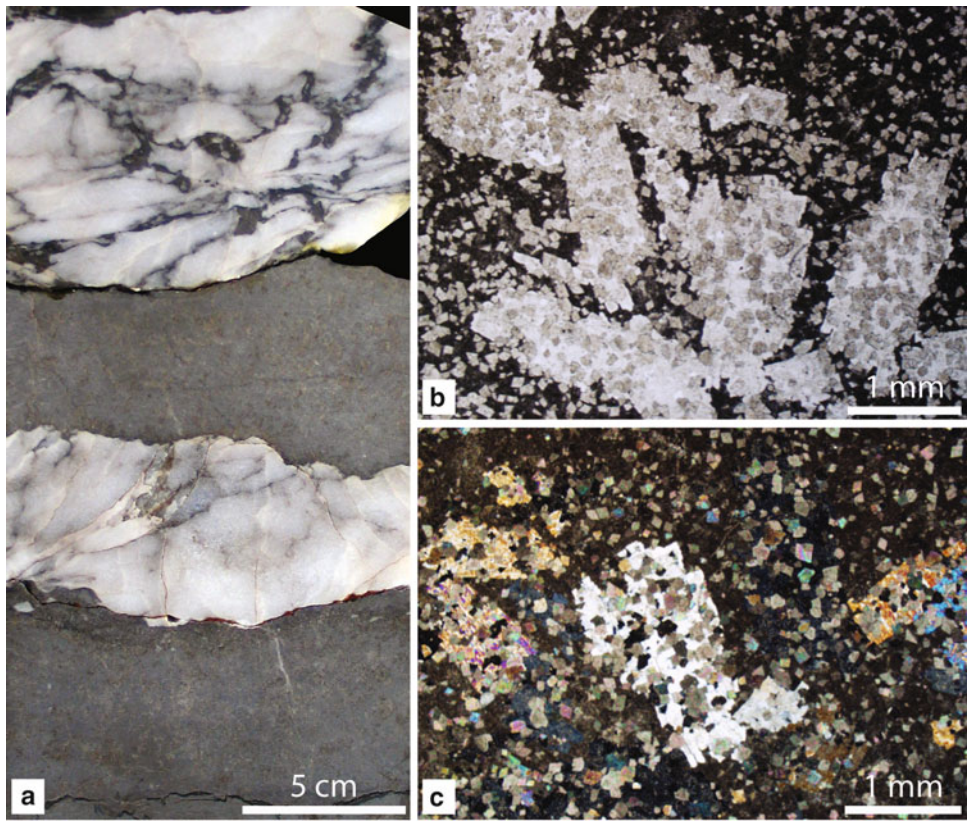

Fig. 21.7 (**a**) Cycles consisting of gypsum-anhydrite-bearing limestone (*gray*) and anhydrite (*white*) with chicken wire fabric. (**b**–**c**) Photomicrographs of the gray limestone portion in (**a**) under normal light (**b**) and under polarized light (**c**), showing scattered crystals and lenticular forms of gypsum and anhydrite in a lime mudstone groundmass. Absence of subaerial exposure features indicates deposition in a subtidal lagoon or in an intertidal pond settings; Upper Jurassic Mozduran Formation in the Kopet Dagh Basin, northeast Iran

lower to middle intertidal settings. Such stratification is common in ancient carbonate tidal deposits (Figs. 21.11 and 21.12a–c) where the sand-sized layers may consist of quartz sandstone (e.g. Y. Lasemi 1986, Y. Lasemi et al. 2008; Ghomashi 2008) or grainstone (e.g., Demicco 1983; Amin-Rasouli 1999) indicating deposition by high energy ebb or flood tidal currents. The muddy dolomudstone or lime mudstone layers represent deposition by the waning current during the slack water period of a tidal cycle. It may be mud-cracked (Fig. 21.12a) or bioturbated by organisms leaving vertical to sub-horizontal traces (Fig. 21.12c). Periodic pumping of water by tidal currents through lowermost intertidal carbonate sands and subsequent evaporation, results in cementation and formation of a lithified crust known as beachrock (Scoffin and Stoddard 1983) (Fig. 21.13a, b).

A feature diagnostic to tidal flat environments is birdseyes (fenestral fabric), which are millimeter-size irregular voids and occur in stromatolite structures and carbonates ranging from grainstone to mudstone in texture (Figs. 21.6f, 21.14 and 21.15). They are commonly filled with cement (Figs. 21.6f and 21.15) or geopetal internal sediment (Fig. 21.14a). Birdseyes commonly form as a result of air or gas bubble formation, desiccation shrinkage, wrinkles in the laminated bacterial deposits or development of trapped air bubbles in the pore spaces during flood tide and subsequent rapid cementation (Shinn 1983b, 1986).

The lower intertidal/beach ridge facies of mainland coasts with high salinity conditions are normally characterized by packstone-grainstone facies containing peloids, intraclasts and/or a restricted range of bioclasts, commonly small gastropods (Fig. 21.13b).

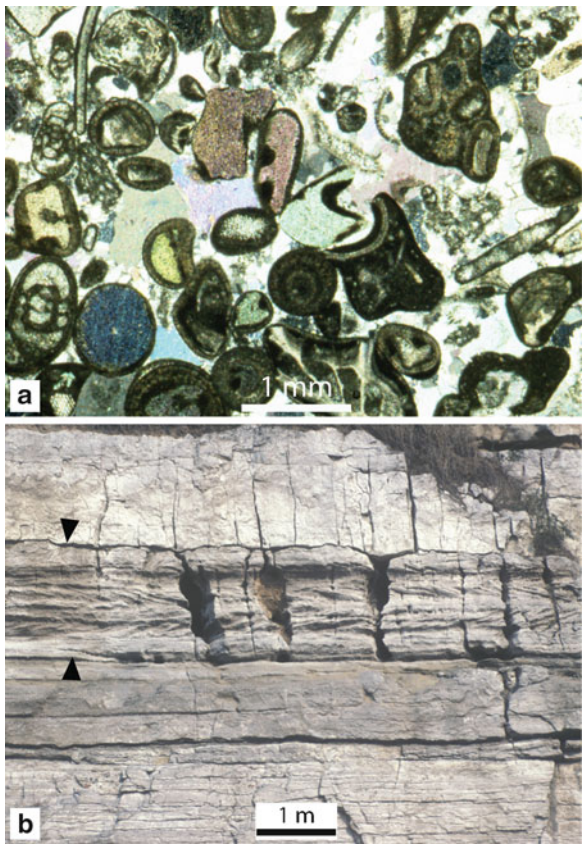

Fig. 21.8 High energy beach and platform margin tidal channel facies: (**a**) Photomicrograph of a bioclastic ooid intraclast grainstone under polarized light; Mississippian upper Salem Limestone (lower St. Louis Limestone equivalent), southwestern Illinois. (**b**) A fining-upward ramp margin tidal channel deposit (*lower arrow* at the basal erosional contact) within a predominantly ooid grainstone sequence. Note that facies of this channel deposit include flat-bedded and laminated gravel- to sand-sized ooid intraclast grainstone overlain by herringbone cross-bedded grainstone, which in turn grades to laminated ooid grainstone. The channel deposit is overlain, with a sharp contact (*upper arrow*), by rocks of a transgressive open marine mudstone facies; Mississippian Ste. Genevieve Limestone, Alton Bluff section, Madison County, southwest Illinois

These sediments, similar to a beach facies (Inden and Moore 1983), commonly are characterized by fenestral grainstone facies (e.g. Y. Lasemi 1995) (Figs. 21.14 and 21.15c). Prolonged exposure in arid to semiarid climate leads to partial dissolution of carbonate grains by meteoric water, pore enlargement, and formation of iron oxide stained coated grains (Fig. 21.14c).

In protected modern and ancient Phanerozoic Humid intertidal deposits, lamination and other diagnostic features are absent due to intense bioturbation by metazoans (see the Ordovician example in Sect. 21.7.3). In arid climate similar to the southern part of the Persian Gulf (Fig. 21.2a), however, due to high salinity and evaporite formation, burrowers and browsers are practically absent in the upper intertidal deposits, whereas, the lower intertidal facies are intensely bioturbated. These deposits, except for their lower fossil diversity and lighter color due to more oxidizing condition, are similar to the adjacent subtidal deposits (Shinn 1983a).

The low energy and isolated intertidal pond facies is thin bedded and laterally discontinuous. In a humid condition, it is characterized by thin beds of bioturbated lime mudstone to wackestone containing restricted-bioclast. In an arid climate, the pond facies may consist of planar stromatolite (Fig. 21.16a) and/or evaporitic dolomudstone, depending on geographical location and salinity. Intertidal channel point bar deposits are characterized by erosive based fining-upward gravel- and sand-size sediment (may be laminated and/or herringbone cross-bedded) skeletal intraclast/peloid grainstone to packstone facies. They are laterally discontinuous and normally are capped by intertidal deposits (Fig. 21.16b, c).

21.5.3 Supratidal Belt

Sediment of the supratidal environment is transported from the subtidal carbonate factory during spring and storm tides. Because most of the sediment is carried by storms that transport large quantities of sediment, carbonate facies of the supratidal belt are intraclastic and commonly are characterized by thick laminae and thin to very thin beds (Figs. 21.17a, b, d and 21.18c). Periodic exposure of muddy tidal flat deposits particularly in the upper intertidal and supratidal settings results in desiccation and the formation of mud cracks and mud polygons (Figs. 21.3a, b, 21.9d, 21.12a, and 21.17). These cracks are strikingly different than diastasis cracks (Cowan and James 1992) that result from differential mechanical behavior of stiff muddy sediment, under stress, in any subtidal environment. Desiccation cracks may show a variety of sizes depending on exposure time, layer thickness, and the presence or absence of microbial mats (Shinn 1986). Mud cracks in carbonates may develop a variety of cross-sectional shapes ranging from classical "v" to wide and parallel-walled or deep

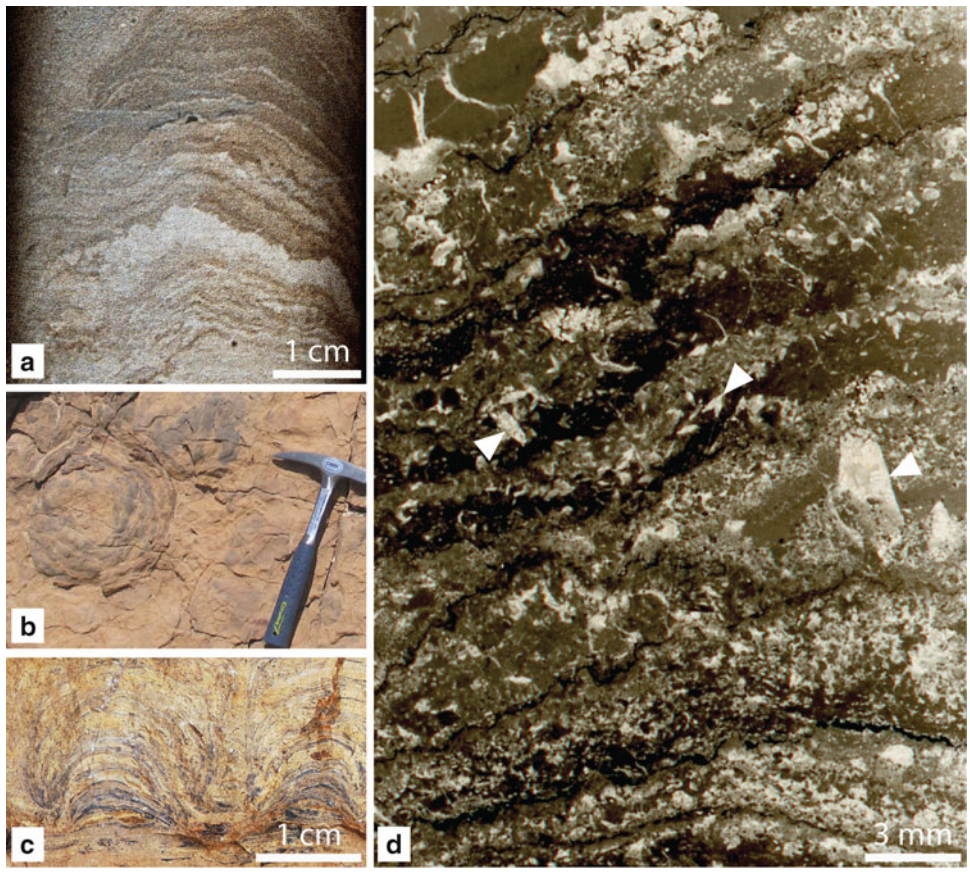

Fig. 21.9 Intertidal stromatolites: (**a**) Core photograph from a dolomitized wavy to domal intertidal stromatolite; Middle Devonian Grand Tower Limestone, Tuscola Quarry, Douglas County, east-central Illinois. (**b**–**c**) Photographs from the upper bedding plane (**b**) and vertical section (**c**) of a domal lower intertidal stromatolite; Middle Cambrian member 2 of the Mila Formation in central Alborz Mountains, northern Iran. (**d**) Thin section photograph showing mud-cracked wavy stromatolite with calcite pseudomorphs after gypsum crystals (*arrows*). Note the disrupted laminae throughout the sample as a result of desiccation and crystal growth. Note also the geopetal vadose sediment inside a gypsum crystal mold in the middle right; Cave Hill Member of the Mississippian Kinkaid Formation, western Kentucky

and narrow shapes. These cracks typically are filled with sediment or carbonate cement (Demicco and Hardie 1994) and their walls are not generally smooth (Figs. 21.3a, b, 21.9d, 21.12a and 21.17a, b, d). In the supratidal facies, as a result of prolong exposure, desiccation related polygonal mud cracks (Figs. 21.3b and 21.17) are larger than those found in the arid upper intertidal belt and on supratidal beach ridges and levees.

Modern and ancient arid supratidal deposits generally comprise dolomudstone which may be interbedded with gypsum/anhydrite and collapse breccias (see the Mississippian, Middle Triassic and Miocne examples in Sects. 21.7.4, 21.7.5.2 and 21.7.6). The dolomudstone layers are commonly fenestral and may contain lenses, nodules or rosettes of gypsum/anhydrite or their pseudomorphs (Figs. 21.15a, b and 21.18). Halite crystals cast (Fig. 21.19c) may be present, but are not always indicative of supratidal conditions (see the Middle Cambrian tidalites in Sect. 21.7.2). In arid supratidal sediment, microbial boundstone is normally absent or occurs as thin crinkly and discontinuous laminae (Fig. 21.17b) due to dry climate, prolonged exposure and wind energy as opposed to humid supratidal setting. The supratidal freshwater marsh facies in humid climates, such as the rainy tidal flats of the Bahamas (Fig. 21.2b), on the other hand, is characterized by interlayered planar to wavy laminated

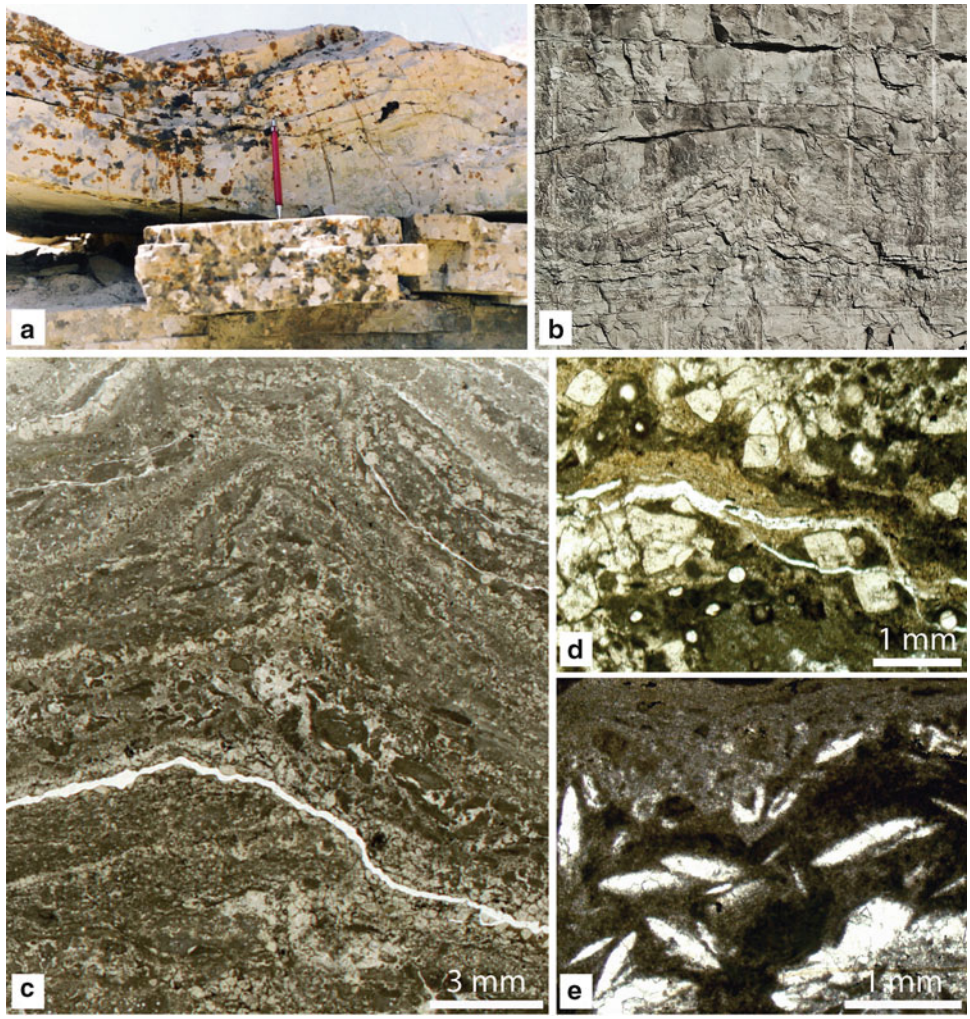

Fig. 21.10 Tepee structures and calcite pseudomorphs after lenticular gypsum: (**a**) Tepee structure in thin-bedded and laminated rocks of the tidal flat facies; Middle Triassic member 2, Elika Formation, eastern Alborz Mountains, northern Iran (scale is 14 cm long). (**b**) A tepee structure (center of the photograph) in a tidal flat succession; lower part of the Mississippian lower St. Louis Limestone at Bussen Quarry, St. Louis County, Missouri. The height of the teepee is about 50 cm. (**c**) Photograph of a thin section from an arid upper intertidal planar stromatolite showing a small tepee structure; Cave Hill Member, Mississippian Kinkaid Formation, Buncombe Quarry, southern Illinois. Note that all the light crystals are calcite pseudomorphs after lenticular gypsum as seen in (**d**). Note also the disruption of the laminae as a result of desiccation and gypsum formation. (**d**) Photomicrograph of a part of sample (**c**) under normal light showing calcite pseudomorphs after lenticular gypsum, microbial laminae and microcrystalline dolomite. Circular objects in the dark microbial laminae are calcispheres believed to be green algal sporangium. (**e**) Photomicrograph under normal light of a microbial lamina containing calcite pseudomorphs after gypsum covered by a sediment-rich lamina composed of intraclastic dolomudstone; Cave Hill Member, Mississippian Kinkaid Formation, Kinkaid Creek section, southern Illinois

stromatolities that typically display fenestral fabric, root casts, desiccation cracks and storm-generated deposits (e.g. Shinn 1986). A well preserved humid tidal flat and the associated coastal marsh facies has been described by Mitchell (1985) from the Middle Ordovician St. Paul Group in central Appalachians (see Sect. 21.7.3). Deposition of calcium carbonate and/or gypsum in tidal flat environments leads to the formation of early diagenetic microcrystalline dolomite by either direct precipitation or replacement of the previously deposited calcium carbonate (e.g. Hardie 1987, Z. Lasemi et al. 1989).

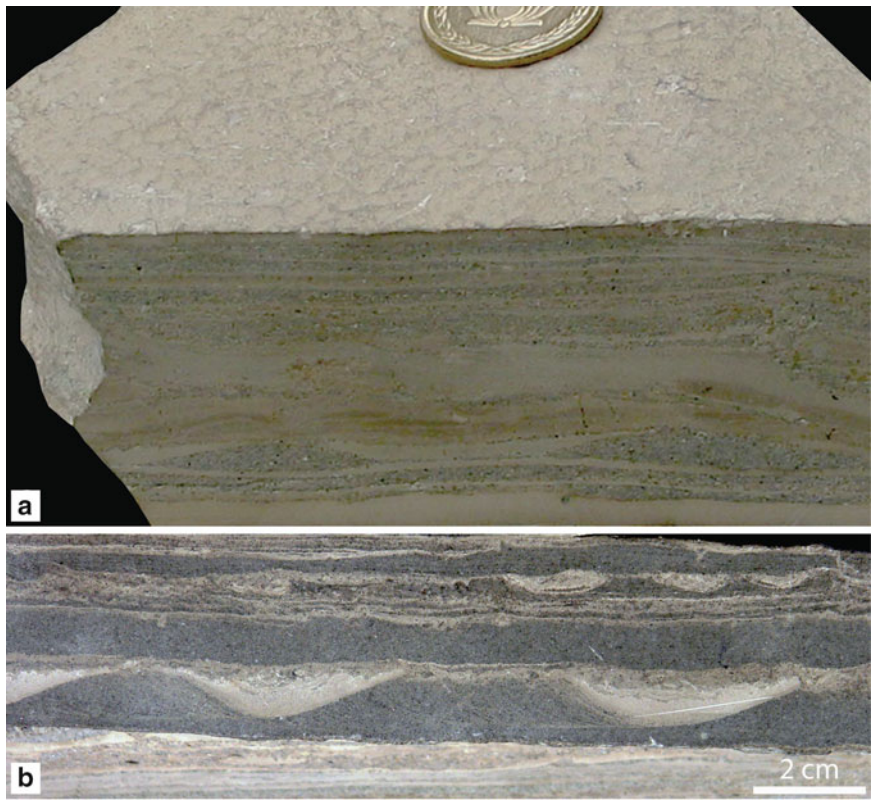

Fig. 21.11 Photographs of hand specimens showing millimeter- to centimeter-scale interlayering of quartz sand (*gray*) and mud-sized carbonate (*tan*) (heterolithic stratification) in the lower part of the Mississippian Bayport Formation, Bayport, Michigan. (**a**) Lenticular and wavy bedding of quartz sand in carbonate mud laminae in the lower part, changing upward to finer scale lamination. Note rain drop impressions in the carbonate lamina on the top of the specimen (*coin* diameter is 2.5 cm). (**b**) Interlayered planar- to wavy-bedded and rippled quartz sandstone (*dark gray*) and carbonate mud laminae (*light gray* to tan). The ripple in the *lower part* of the photograph and its internal trough cross-lamination indicate tidal current direction (possibly flood tide) to the right. Note also that the smaller current ripples in the upper right indicate tidal current reversal (ebb tide). In both ripples carbonate mud fills the ripple troughs forming flaser bedding

Other features common in supratidal setting include very thin lenticular bedding (Fig. 21.17b), root casts (Fig. 21.15b), rain drop impressions (Fig. 21.11a) and tepee structures (see the previous section). The supratidal facies may be capped by wind-blown bimodal and super-mature quartz sandstone (Fig. 21.19d) during seaward progradation (see the Lower Triassic tidalites in Sect. 21.7.5.1). The supratidal facies of beach ridges and channel levees (Fig. 21.2b) are laterally discontinuous and have a very low preservation potential. They consist of very thin bedded, interlaminated mud cracked fenestral mudstone laminae with a thin microbial coating and crinkly stromatolite boundstone (Shinn 1986).

21.6 Peritidal Cycles and Sequence Stratigraphy

The peritidal facies commonly are arranged into meter scale, shallowing-upward successions of subtidal- to tidal flat facies (e.g. Wilson 1975; James 1984; Hardie and Shinn 1986; Grotzinger 1986b, 1989; Pratt et al. 1992; Pratt 2010). In a single shallowing-upward cycle, facies boundaries are transitional in accord with Walther's Law (for an example see figure 21.21a), and the contact between the shallow-water and deeper facies of the overlying cycle is erosional or sharp due to non-deposition or prolong exposure (Fig. 21.21a, b).

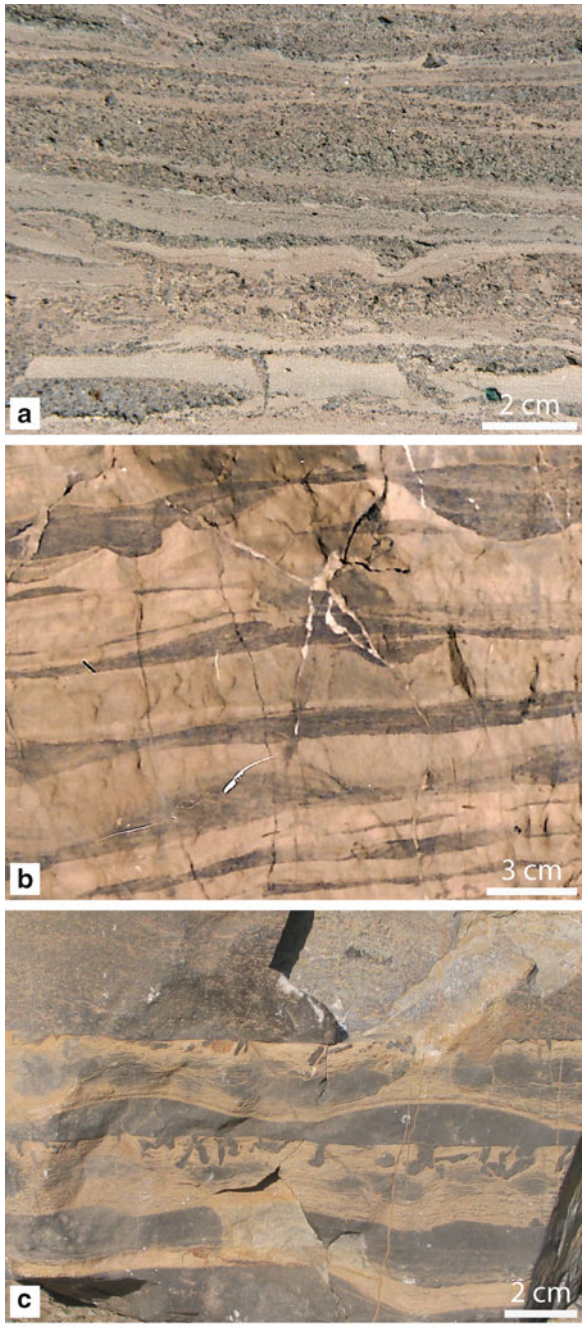

Fig. 21.12 Planar, wavy and ripple bedding in mixed carbonate-siliciclastic and pure carbonate intertidal deposits: (**a**) Millimeter- to centimeter-thick tidal lamination in interlaminated lime mudstone and quartz sandstone (*gray*). Note disrupted laminae, intraclasts, smooth-walled sand-filled desiccation cracks and lenticular bedding in the lower part; Mississippian Bayport Formation, Bayport, Michigan. (**b**–**c**) Intertidal heterolithic interlayering of dolomudstone and grainstone in the Middle Cambrian member 2 of the Mila Formation from the Alborz Mountains, northern Iran: (**b**) Interlayered wavy and rippled grainstone and dolomudstone containing lenticular bedding. (**c**) Wavy, ripple and lenticular bedding. Note the vertical and sub-vertical burrows in the middle of the photograph that was filled during the deposition of the overlying current ripple. The uppermost layer is a bioclastic intraclast grainstone transgressive lag deposit

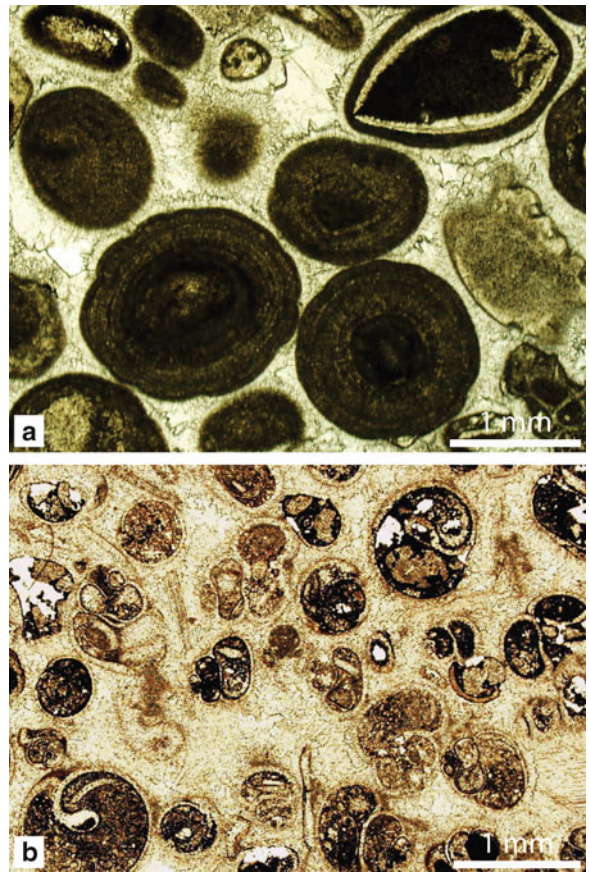

Fig. 21.13 (**a**) Fibrous and irregular sparry calcite cement fringes (beachrock cement) in a bioclastic ooid grainstone interpreted as a barrier beach facies; Upper Mississippian Negli Creek Member of the Kinkaid Formation, southern Illinois. (**b**) An example of a beach ridge grainstone composed solely of small gastropod shells with void-filling hematite and calcite cements. Note the irregular radial fibrous beachrock cement fringe on the grains; Lower Triassic lower member of the Elika Formation in the central Alborz Mountains, northern Iran

Even though shallowing-upward cycles dominate the peritidal successions, deepening-upward and deepening- to shallowing-upward trends or aggradational cycles consisting of a single facies are also present (see Fig. 21.3d for an example) (e.g. Burgess 2006; Spence and Tucker 2007; Bosence et al. 2009; Zecchin 2010) depending on rates of deposition and sea level fluctuations during the course of their development. Some ancient successions consist of stacked cycles characterized by a subtidal facies capped by karstic or calichie

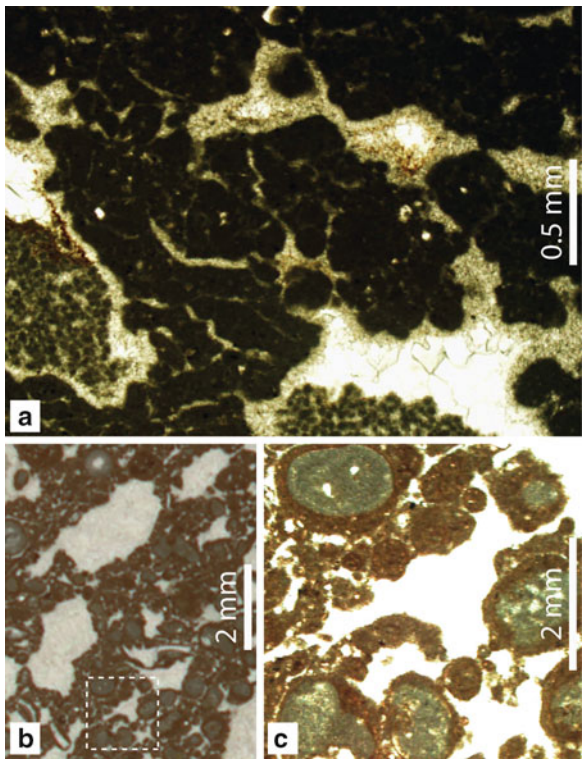

Fig. 21.14 (**a**, **b**, **c**) Subaerial exposure features in intertidal fenestral grainstone from the Upper Jurassic Mozduran Formation in the Kopet Dagh back arc basin, northeast Iran: (**a**) Photomicrograph under normal light of a fenestral peloidal intraclast grainstone. Note that the geopetal sediment (silt-sized peloids) overlies earlier *light brown* vadose cement and is overlain by late stage phreatic drusy mosaic cement. (**b**–**c**) Thin section photograph of fenestral grainstone facies showing subaerial exposure features. Photograph (**c**) is the enlarged portion of the *lower part* of (**b**) showing partial dissolution of the grains, enlarged pores and formation of iron oxide stained coated grains

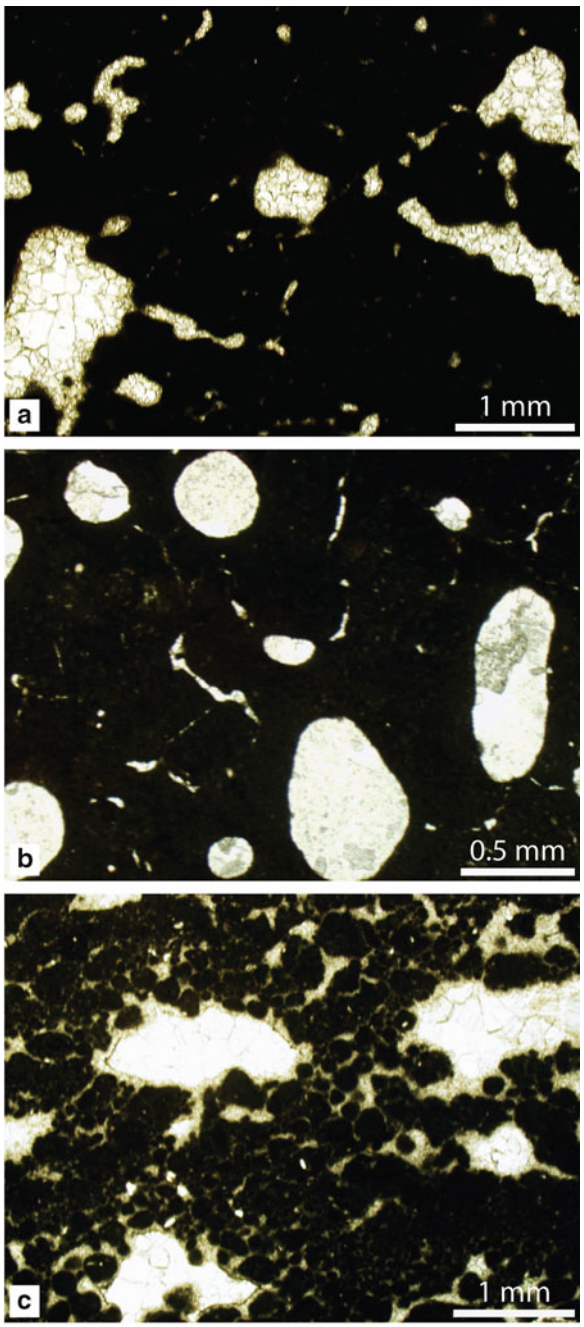

Fig. 21.15 (**a**, **b**) Photomicrographs of calcite cemented fenestral fabric (birdseyes) in lime mudstone interpreted as supratidal facies. Note the calcite-cemented root casts and small birdseyes in b; Cave Hill Member of the Mississippian Kinkaid Formation, southern Illinois. (**c**) Photomicrograph of the lowermost intertidal calcite-cemented fenestral peloid intraclast grainstone under plane-polarized light showing early vadose cement (*light yellowish brown crystals*) that lines the larger fenestrae and fills the smaller voids. Note that the vadose cement is overlain by later phreatic cement indicating subaerial exposure; Upper Jurassic Mozduran Formation in the Kopet Dagh back arc basin, northeast Iran

soil horizon without any intervening tidal flat facies as a result of rapid sea level fall and prolonged exposure (Hardie 1986; Preto et al. 2004). Examples include the karstic soil-capped cycles of the Plio-Pleistocene deposits of the Bahamas (Beach and Ginsburg 1980) and the calichie-capped tepee dominated diagenetic cycles of the Middle Triassic Latemar Limestone of northern Italy (Hardie et al. 1986) formed under humid and arid- to semiarid conditions, respectively. The meter-scale peritidal cycles are known as parasequences (e.g., Van Wagoner et al. 1988; Lehrmann and Goldhammer 1999; Burgess 2006; Spence and Tucker

Fig. 21.16 (**a**) Photomicrograph of a bioturbated ostracod dolomudstone with microbial laminae from an intertidal flat sequence interpreted as the intertidal pond facies; Mississippian Bayport Formation, Bayport, Michigan. (**b, c**) Intertidal channel deposits from the Middle Triassic middle member of the Elika Formation in east central Alborz Mountains, northern Iran. (**b**) Erosive-based fining-upward intertidal channel sequence (*arrow* at the erosional contact) composed of a grainstone bed with gravel-size intraclasts grading upward into a trough cross-bedded sand-size grainstone that in turn grades to herringbone cross-bedded grainstone (*above the scale*) covered by an intertidal deposit (pen for scale is 14 cm long). (**c**) A tidal channel deposit (pen on the left side of the channel facies is 14.5 cm long) within a laminated and thin-bedded tidal flat succession. Note that the channel facies thins to the *right* of the photograph and pinches out completely toward the *left*

2007; Catuneanu et al. 2009), the fundamental unit of stratigraphic sequences.

Many ancient peritidal successions, at least in part, lack any stratal order and comprise random vertical facies transition and thickness patterns (e.g. Wilkinson et al. 1997). The random stratigraphic patterns have been interpreted to be the result of deposition in a set of randomly distributed environments (e.g. Wilkinson et al. 1996, 1999). Recent studies (e.g. Lehrmann and Goldhammer 1999; Lehrmann and Rankey 1999; Spence and Tucker 2007) and investigation on the Holocene carbonates of the Bahamas (Rankey 2002), on the other hand, indicate highly ordered facies transitions in peritidal facies tracts and the resulting vertical successions. The random facies patterns in ancient successions may have been the consequence of incomplete stratigraphic record and extrabasinal forcing mechanisms (Rankey 2002; Lehrmann and Goldhammer 1999). Random vertical successions normally develop during icehouse conditions, due to unfilled accommodation space created by higher-frequency, higher-amplitude sea level changes (Lehrmann and Goldhammer 1999; Burgess 2006).

21.6.1 Origin of Meter-Scale Cyclicity

Shallowing-upward cycles form when tidal flats aggrade to sea level and prograde into the adjacent subtidal setting. This is the consequence of high sedimentation rate in tidal flat areas that normally exceeds the available accommodation space created by high-frequency 5th- to 4th-order sea level rise. Progradation leads to a seaward thickening wedge of tidal flat sediments and a succession of subtidal- to intertidal- to supratidal facies (e.g. Hardie 1986). Repeated deepening and filling of accommodation space in response to relative sea level changes (the sum of eustatic sea level change, subsidence and sediment supply), lead to

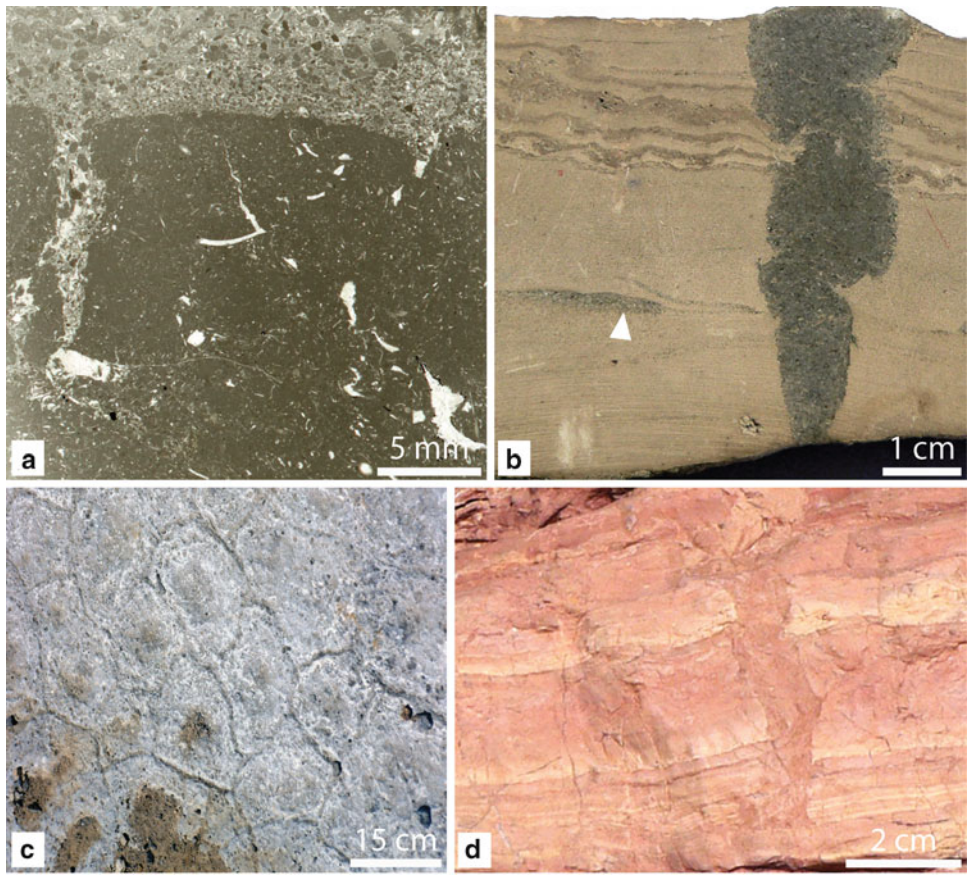

Fig. 21.17 Desiccation cracks in laminated supratidal sediment: (**a**) Sediment filled mud crack in a peloid wackestone lamina covered by an intraclast grainstone transgressive lag deposit; Cave Hill Member of the Mississippian Kinkaid Formation, southern Illinois. (**b**) Quartz sand-filled 'V' shaped mud crack in a mixed carbonate-siliciclastic tidal flat sequence. Note the irregular wall of the crack and a small quartz sand-filled lenticular bed (*dark gray*) in thickly-laminated dolomudstone toward the *middle* of the *left side* of the photograph. Fine-scale laminations in the *upper part* comprise dark crinkly stromatolite and dolomudstone laminae. (**c**) Plan view of mud cracks in the upper surface of a supratidal deposit; Mississippian lower St. Louis Limestone, Columbia Quarry, St. Clair County, southwest Illinois. (**d**) Dolomudstone-filled mud crack in tan to *pink laminated* deposits of the supratidal facies (Photo courtesy of Dr. M. Ghomashi, Sistan-Baluchistan University, Zahedan, Iran); Lower Triassic Sorkh Shale Formation, Tabas failed rift basin, east central Iran

stacked complete and incomplete meter-scale successions (see the illustrative examples). Progradation to develop stacked peritidal meter-scale cycles can be generated by intrabasinal autocyclic processes and extrabasinal allocyclic mechanisms including eustatic sea level fluctuation and tectonic subsidence (e.g., Hardie 1986; Pratt et al. 1992; Pratt 2010).

21.6.1.1 Autocyclicity

Autocycles form in response to processes operating within the environment of deposition and include tidal flat shoreline and island progradation and lateral migration of tidal channels. Tidal flat progradation is the dominate process during greenhouse periods (small polar ice volume) due to lower-amplitude high-frequency sea level changes (Lehrmann and Goldhammer 1999; Burgess 2006). Tidal flat shoreline progradation to generate stacked shallowing-upward peritidal cycles (Ginsburg 1971; Hardie 1986) assumes gradual subsidence, slow sea level rise or stillstand and changes in sedimentation rate during deposition. High sedimentation rate in tidal flat areas results in progradation

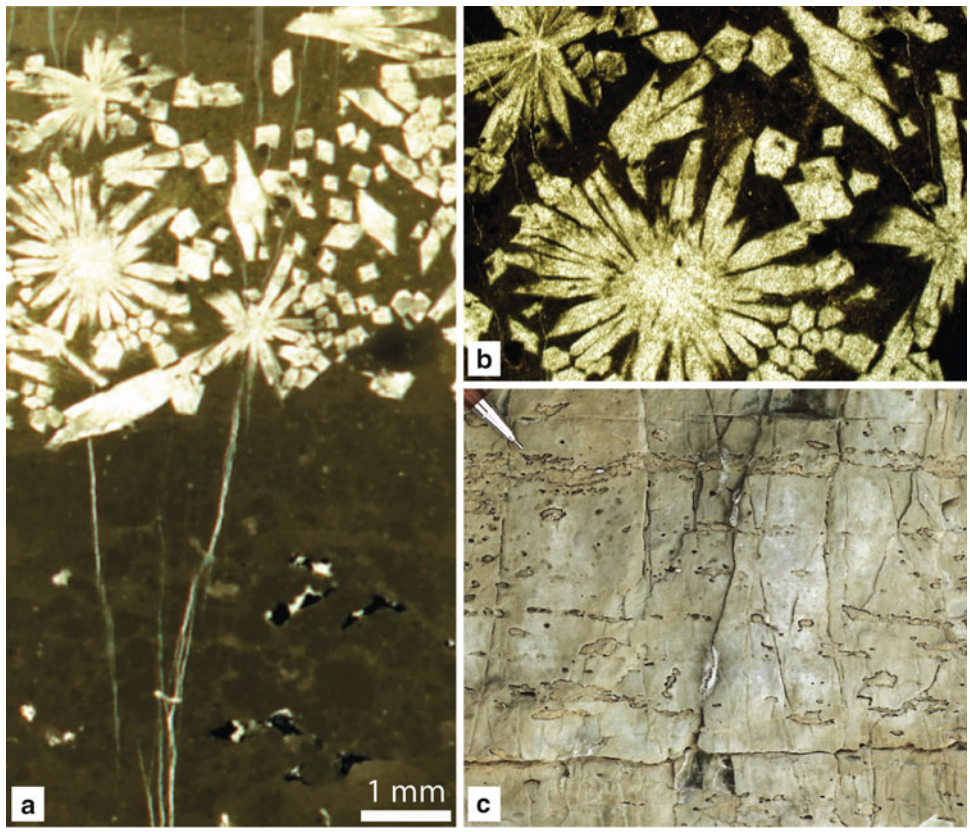

Fig. 21.18 Supratidal facies: (**a**–**b**) Rosettes and laths of calcite pseudomorphs after anhydrite within a fenestral lime mudstone from the Cave Hill Member of the Mississippian Kinkaid Formation, southern Illinois. Note that in a (thin section photograph) birdseyes are almost totally filled with vadose silt. Note also that in (**b**) (photomicrograph of the enlarged portion of the *upper left* of (**a**) under normal light) the rosettes are filled with coarsely crystalline calcite cement. (**c**) Field photograph of a thickly laminated fenestral dolomudstone containing lenticular gypsum casts (the silver end of the pen in the upper left is 3 cm long); Middle Triassic middle unit of the Elika Formation in the Ghoznavi section, eastern Alborz Mountains, northern Iran

and rapid infilling of the subtidal carbonate factory. Subsidence and subsequent sea level rise result in the resumption of carbonate deposition (after a lag period) and formation of a new asymmetric shallowing-upward cycle. An alternative autocyclic mechanism, the tidal flat island model, has been proposed for peritidal shallowing-upward cycles that are laterally discontinuous (Pratt and James 1986; Pratt 2010). In this model, deposition would take place on small low relief islands and intertidal banks separated by subtidal source areas. Progradation and lateral growth of the islands may generate shallowing-upward peritidal cycles of limited areal extent with random stratigraphic distribution and variable thicknesses (Pratt et al. 1992; Pratt 2010).

Lateral migration of tidal channels is another autocyclic process forming discontinuous small-scale cycles. Migration of intertidal channel leads to point bar deposits which are laterally discontinuous, erosive-based, fining-upward successions of gravel- and sand-size sediments capped by a laminated tidal flat facies (Fig. 21.16b, c). Tidal channel migration in platform margin shoals generates an erosive-based fining-upward succession (Fig. 21.8b), capped by offshore, tidal flat, lagoonal or coarsening-upward beach facies (Inden and Moore 1983).

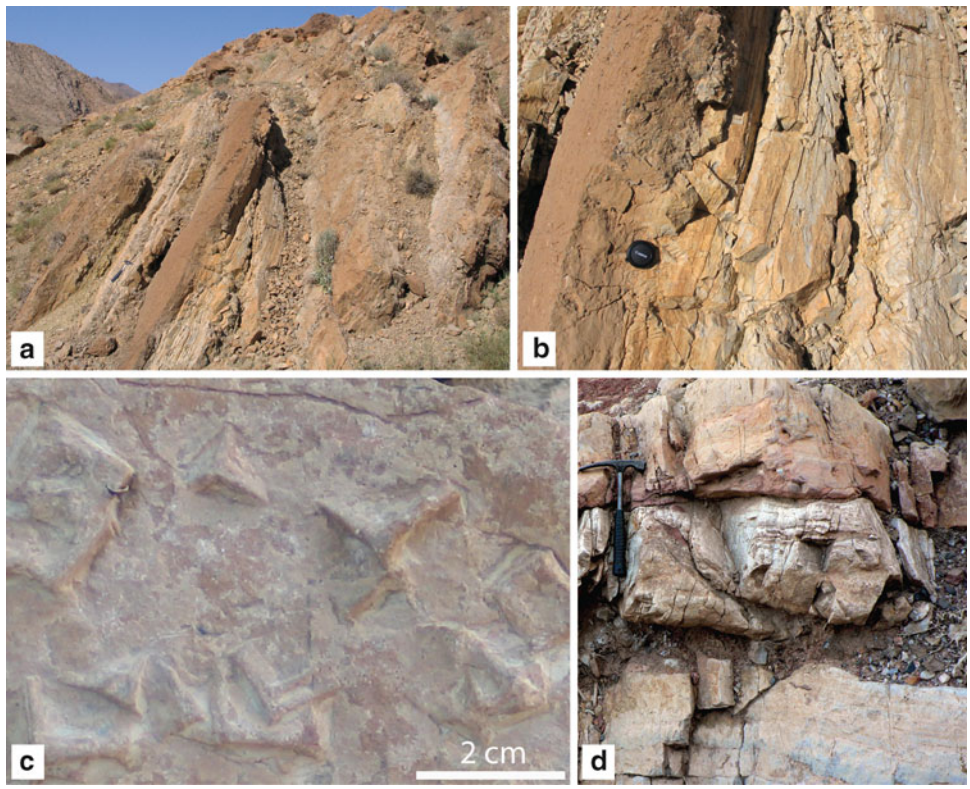

Fig. 21.19 (**a**) Interlayered *light green*- to *reddish brown* laminated argillaceous dolomudstone/dolomitic shale and *reddish brown* and fine- to very fine-grained lithic sandstone from the Middle Cambrian member 2 of the Mila Formation, eastern Alborz Mountains, northern Iran. (**b**) Close up view of a part of (**a**) showing the laminated shale/dolomite and the capping sandstone facies (Lens cap diameter is 5.5 cm). The laminated shale-carbonate facies contain hopper halite casts and has no subaerial exposure features interpreted as a lowstand coastal salina pond deposit. (**c**) Cast of hopper halite crystals mentioned in (**b**). (**d**) A laminated supper mature quartz arenite bed overlies and underlies, with abrupt contacts, a fenestral dolomudstone (supratidal facies) forming a pure carbonate and pure siliciclastic double cycle (Y. Lasemi et al. 2008); base of the transgressive systems tract in the Lower Triassic Sorkh Shale Formation, south of the Tabas failed rift basin, east central Iran

21.6.1.2 Allocyclicity

In many ancient carbonate tidalites, cyclicity has been interpreted based on Milankovitch-band periodic climate changes (e.g. Goldhammer et al. 1987; Koerschner and Read 1989; Goldhammer et al. 1993; Strasser et al. 1999; Preto et al. 2004). In the Milankovitch orbital forcing model, three parameters including precession, obliquity and eccentricity could generate high frequency eustatic sea level cycles with approximate durations of 20,000, 41,000 and 100,000 years, respectively. Evidence for Milankovitch-band periodic eustatic sea level changes in the stratigraphic record include lateral continuity of cycles on a regional and interregional scale, 5:1 grouping of 5th-order small-scale cycles to form larger 4th-order cycles of 100,000 years duration, and high frequency subtidal cycles with karstic or calichie soil caps (e.g. Goldhammer et al. 1987; Koerschner and Read 1989; Preto et al. 2004). Allocyclicity is strong during icehouse periods due to higher-amplitude relative sea level changes (Lehrmann and Goldhammer 1999; Burgess 2006).

Subsidence due to high-frequency extensional fault movements ("yo-yo" and "yo" tectonics) can also create accommodation space for the formation of stacked peritidal cycles (Hardie 1986; Hardie et al. 1991; De Benedictis et al. 2007; Bosence et al. 2009). According to Bosence et al. (2009), the cycles form due to filling of accommodation created by episodic rapid downwarping followed by slow subsidence in the hanging wall and graben sites ("yo" tectonics) and concurrent rapid uplift and slow subsidence in the footwall sites ("yo-yo" tectonics). The most common cycle type is asymmetric shallowing-upward, but symmetric deepening then shallowing-upward, asymmetric

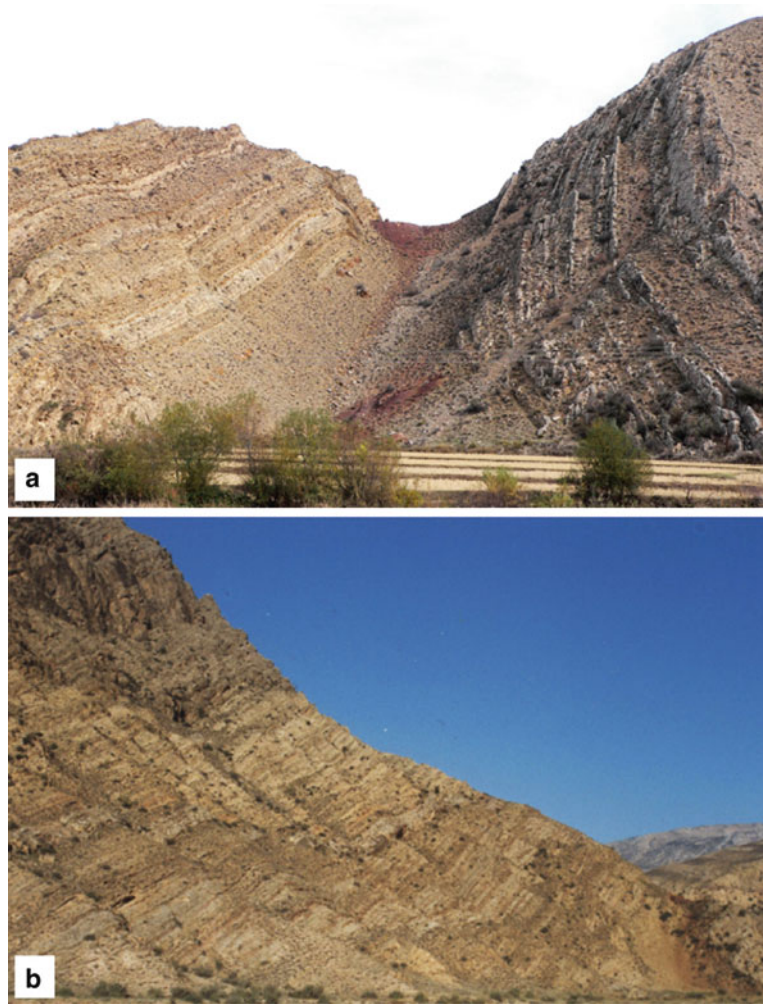

Fig. 21.20 Panorama of conspicuously bedded peritidal carbonate successions along the Azadshahr Highway in eastern Alborz Mountains: (**a**) Highstand lagoonal shallowing-upward cycles of the Upper Permian Ruteh Formation (*right*) capped by a laterite horizon, which is in turn overlain by the peritidal cycles of the Lower Triassic lower member of the Elika Formation. (**b**) The Lower and Middle Triassic peritidal deposits of the lower and middle members of the Elika Formation comprising two depositional sequences. The lower sequence is bounded by the lowstand laterite horizon at the Permian-Triassic boundary (*right*) and a quartz sandstone bed at the Lower-Middle Triassic boundary in the middle of the photograph, and consists of lagoonal- to intertidal cycles intercalated by numerous storm beds. The Middle Triassic middle member (*upper left* of the photograph) is a depositional sequence composed almost entirely of intertidal- to supratidal shallowing-upward cycles

with subaerial exposure surface or karstic/calichie soil cap, and asymmetric deepening-upward can develop depending on tectonic setting. The cycles have the same thickness and frequency as eustatic or autocyclic processes, however, lateral variation of cycle types and cycle stacking and irregular non-bundled stacking of the cycles support an overriding tectonic control (De Benedictis et al. 2007; Bosence et al. 2009).

21.6.1.3 Sequence Stratigraphy

The meter-scale cycles are superimposed on an underlying lower-frequency 3rd-order relative sea level cycle (e.g. Goldhammer et al. 1993; Kerans and Tinker 1997; Spence and Tucker 2007) (see the Middle Triassic tidalites in Sect. 21.7.5.2 for an example). The 3rd-order cycle has a duration of 1–3 my (Haq et al. 1987) or 1–10 my, (Kerans and Tinker 1997; Lehrmann

Fig. 21.21 (**a**) Brownish gray lagoonal deposits (*right*) grading into *light brown* intertidal and supratidal deposits. Note the abrupt upper contact (*dashed line*) with the overlying lagoonal deposit (the *encircled tree* is about 3 m tall); Lower Miocene middle member of the Asmari Formation in the Mish Mountain, Zagros Mountain range, southwest Iran. (**b**) *Dark gray* bioturbated lime mudstone (subtidal lagoon facies) overlies, with an erosional contact, a *yellow* dolomudstone (tidal flat facies) indicating transgression over a tidal flat cycle cap; Lower Triassic lower member of the Elika Formation in the central Alborz Mountains, northern Iran

and Goldhammer 1999) and represent a depositional sequence. A depositional sequence as defined by Mitchum et al. (1977) is a stratigraphic unit composed of a relatively conformable succession of genetically related strata bounded by unconformities (Fig. 21.20) or their correlative conformities. Catuneanu et al. (2009) recommended using the term 'stratigraphic sequence', a sedimentary succession deposited during a full cycle of change in accommodation or sediment supply (Fig. 21.22), which is compatible with various existing sequence stratigraphic models (For a detailed review of sequence stratigraphic principles and models see Miall 1997; Schlager 2005; Catuneanu 2006; Catuneanu et al. 2009).

A depositional sequence can be subdivided into systems tracts (linkage of contemporaneous depositional systems) as defined by Brown and Fisher (1977), which are defined on the basis of parasequence stacking patterns, position within the sequence and types of bounding surfaces (Van Wagoner et al. 1988, 1990). A depositional sequence may consist of up to four types of systems tracts depending on the shape of base-level curve, type of depositional system, basinal setting, and post depositional erosion at the sequence boundary (e.g. Catuneanu 2006; Catuneanu et al. 2009). These packages include lowstand, transgressive, highstand and falling stage systems tracts (Fig. 21.22).

The lowstand systems tract (LST) overlies the sequence boundary and comprises normal regressive sediments deposits after the onset of relative sea level rise. The transgressive systems tract (TST) lies between the transgressive surface (ts) above the LST or it overlies the sequence boundary and is capped by maximum flooding surface (mfs). It forms when the rate of rise exceeds the rate of deposition, displays a deepening-upward facies trend and a characteristic retrogradational parasequence stacking pattern. The highstand systems tract (HST) forms during the late stage of base-level rise, when the rate of deposition exceeds the rate of accommodation being created (shoreline normal regression). HST deposits underlie the FSST or the sequence boundary and are characterized by shallowing-upward facies trend displaying aggradational to progradational parasequence stacking pattern. The falling stage systems tract (FSST) includes the strata deposited during base-level fall (forced regression) and underlies the sequence boundary.

Carbonate platforms produce sediment during periods of base-level rise mainly during transgressive and highstand stages of a base-level curve. During falling stage and lowstand sea level rise, the entire platform or the platform interior is exposed to karstification and calichie (calcrete) development in humid and dry climates, respectively, forming a pronounced subaerial unconformity. Therefore, FSST-LST packages are normally absent and the sequence boundary commonly is capped by transgressive systems tract of the overlying sequence. In a carbonate ramp setting of a passive

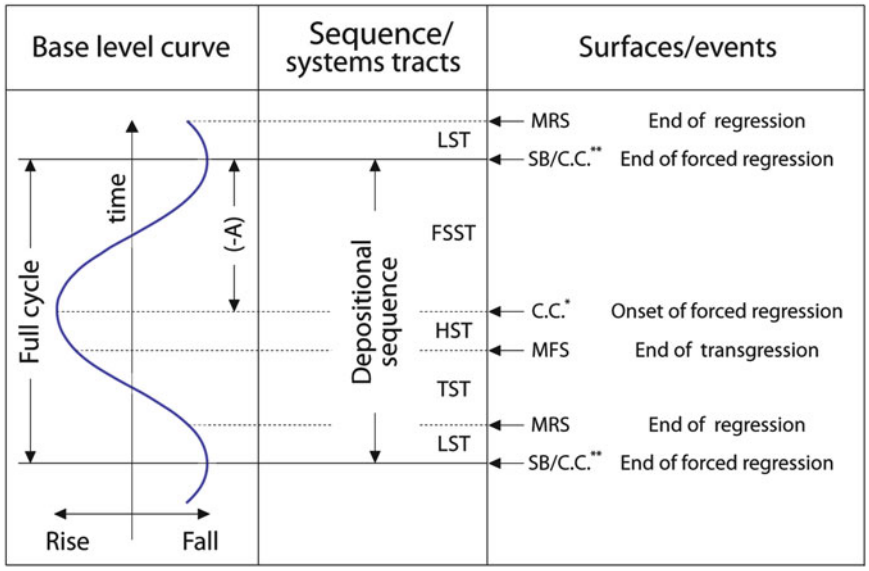

Fig. 21.22 *Base-level curve*, depositional sequence ('stratigraphic sequence'), systems tracts, and sequence stratigraphic surfaces defined in relation to base-level curve (Modified from Catuneanu 2006; Catuneanu et al. 2009). Abbreviations: (**a**), accommodation; *C.C.**, correlative conformity *sensu* Posamentier and Allen 1999; *C.C.***, *sensu* Hunt and Tucker 1992; *MFS* maximum flooding surface, *MRS* maximum regressive surface, SB sequence boundary, *LST* lowstand systems tract, *TST* transgressive systems tract, *HST* highstand systems tract, *FSST* falling stage systems tract

margin succession, however, lowstand peritidal deposits may form during lowstand slow base-level rise consisting of siliciclastics, evaporites or mixed carbonate-siliciclastic peritidal deposits (see the Middle Cambrian tidalites in Sect. 21.7.2 and the Mississippian St. Louis Formation in Sect. 21.7.4).

In mature passive margins, peritidal deposits may constitute the bulk of the transgressive and highstand packages (see the Middle Cambrian and Middle Triassic tidalites in Sects. 21.7.2 and 21.7.5.2). Platform sequences in proximal areas of a basin may consist almost exclusively of tidal flat deposits as in the Lower Triassic Sorkh Shale Formation (see Sect. 21.7.5.1). Sequences in the distal areas of a basin, on the other hand, consist dominantly of subtidal facies with tidal flat facies occurring in the upper part of the highstand systems tracts (see the Lower Triassic Elika Formation in Sect. 21.7.5.1). Absence of peritidal deposits in the transgressive tracts may be the result of rapid base level rise. In foreland basin successions, tidal flat deposits commonly comprise the upper part of the highstand systems tract (see the Miocene tidalites in Sect. 21.7.6); rapid subsidence in response to overthrust loading may prevent tidal flat deposition in the transgressive systems tract.

21.7 Ancient Examples of Carbonate Tidalites

Numerous examples of ancient carbonate tidal facies, practically comparable to their modern counterparts, have been reported from the Precambrian and Phanerozoic successions (e.g. Ginsburg 1975; James 1984; Hardie and Shinn 1986; Tucker and Wright 1990; Demicco and Hardie 1994; Flügel 2010). Ancient carbonate tidalites were deposited on huge carbonate platforms that developed along the Atlantic type passive margins and in smaller platforms associated with failed rifts, intracratonic, foreland, back-arc/fore-arc and pull-apart basins (Read 1985; Grotzinger 1989; Demicco and Hardie 1994). The thickest and most extensive tidal deposits, however, were laid down during Proterozoic through Late Mesozoic times on the vast carbonate platforms that developed along the passive (Atlantic type) continental margins, such as the Iapetus (proto-Atlantic), Paleo-Tethys and Neo-Tethys ocean margins and associated intracratonic basins.

Proterozoic carbonate tidalites consist of microbialites (both thrombolites and stromatolites), ooids, intraclasts and micritic carbonates reflecting carbonate production by chemical and microbial processes.

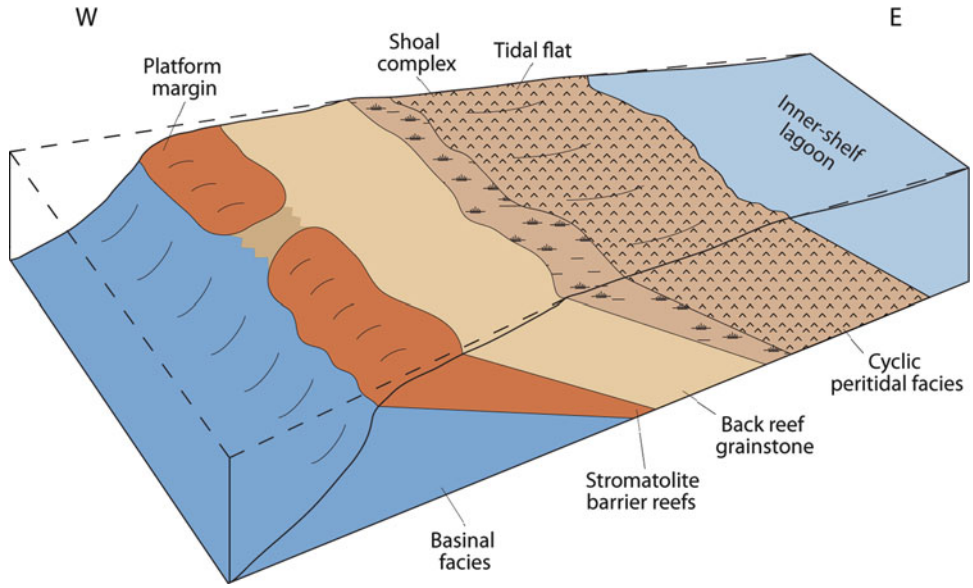

Fig. 21.23 Platform paleogeography during the deposition of the Rocknest Formation (Modified from Grotzinger 1986a). Cyclic peritidal deposits were formed in an extensive back barrier ('*shoal complex*') tidal flat facies setting adjacent to a shallow subtidal lagoon to the east of the platform

These deposits commonly are characterized by the paucity of grainstone facies and the dominance of stromatolite reefs and fine-grained carbonate facies (Grotzinger 1989). During the Precambrian, stromatolites were able to flourish in any setting from deep marine to supratidal and normal to hypersaline waters (e.g. Hoffman 1976; Grotzinger 1989). Although skeletal metazoans were absent prior to Cambrian time, the Precambrian carbonates were deposited in platforms and environments surprisingly similar to those of their Phanerozoic counterparts (e.g. Hardie and Shinn 198, Grotzinger 1989; Flügel 2010).

In the Phanerozoic deposits, in addition to microbialites, micritic carbonates, ooids, oncoids and intraclasts that appeared in the Precambrian platform deposits, various new components, including skeletal grains and fecal pellets emerged. A number of metazoans and calcareous algae constructed patch, fringing and barrier reefs and by late Phanerozoic time seagrass probably contributed in stabilizing mud size sediments in the subtidal setting. During the Phanerozoic, burrowing activity by metazoans and increased supply of sand- to silt-sized bioclasts and peloids restricted microbialites mainly to areas of low sediment influx (Pratt 1982) and to more ecologically stressed environments. The following section of this chapter summarizes facies, paleo-environment, and cycle/sequence stratigraphic analyses of a few specific examples of ancient carbonate tidal deposits representing the Proterozoic through Tertiary successions. The examples represent arid and humid carbonate and mixed carbonate-siliciclastic tidal deposits that occur in various systems tracts of depositional sequences related to passive and active continental margins.

21.7.1 Tidalites of the Rocknest Formation of Northwest Canada

The Lower Proterozoic (older than 1,800 Ma) Rocknest Formation is a carbonate platform succession up to 1,200 m thick that was deposited in a westward-facing passive margin in Northwest Territories, Canada (Grotzinger 1989). This summary describes a back barrier mixed carbonate-siliciclastic peritidal succession (Hoffman 1975; Grotzinger 1985, 1986a, b). In the Rocknest platform, an extensive belt of tidal flat environment developed behind a barrier ('shoal-complex') that separated a wave-dominated windward platform margin to the west from an extensive low energy inner-shelf lagoon to the east (Fig. 21.23). The proximal area of the 'shoal-complex' was seldom

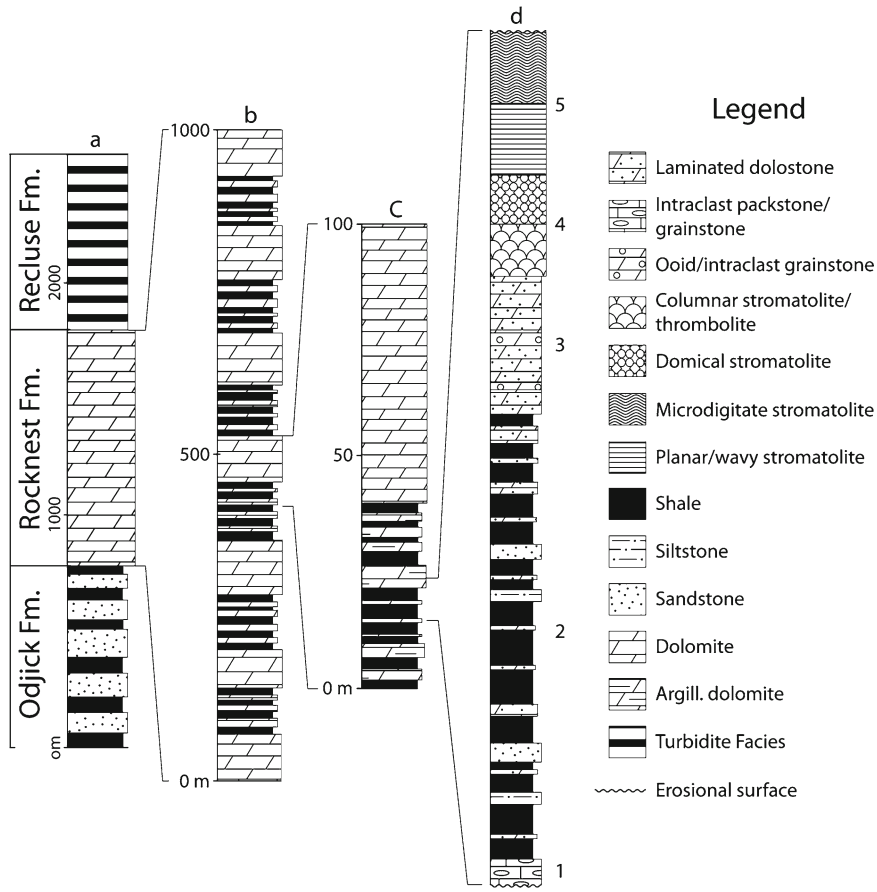

Fig. 21.24 Stratigraphic columns (**a**–**c**) and the peritidal shale-based cycle of the inner shelf cyclic facies (**d**) of the Rocknest Formation in the Lower Proterozoic carbonate platform succession. Numbers 1 through 5 denote lagoonal and tidal flat facies or facies groups within the cycle (Modified from Hoffman 1975 and Grotzinger 1986b). *1*: transgressive lag deposit; *2*: distal inner-shelf lagoon facies; *3*: proximal inner-shelf lagoon facies; *4*: upper subtidal-lower intertidal facies; *5*: upper intertidal-supratidal facies

submerged, preventing communication between the open sea and the low energy inner shelf lagoon. The tidal flat and lagoonal deposits of the Rocknest Formation are characterized by mixed carbonate and siliciclastic facies that grade eastward to siliciclastic deposits.

The Rocknest peritidal facies are arranged into asymmetric shallowing-upward cycles (Fig. 21.24d), which display various basal lithofacies reflecting their paleogeographic location on the platform. Consequently, the shale-based cycles of the distal inner-shelf lagoon pass westward into laminated dolostone-based cycles and stromatolite-based cycles of the 'shoal-complex'. The cycles were initiated by rapid transgression and flooding of tidal flats followed by eastward progradation of the tidal flat facies over the lagoonal facies of the inner shelf during sea level fall. Shale-based cycles up to 15 m thick contain the most diverse facies, which from base to top include (Fig. 21.24d): (1) intraclast packstone to grainstone, 5–30 cm thick that covers erosional tops of cycles and commonly consists of rounded stromatolitic fragments derived from the upper part of the underlying cycle (transgressive lag deposit); (2) mixed carbonate-siliciclastic facies consisting of below- to above-wave-base interstratified argillaceous dolomudstone and shale containing intercalations (up to 30 cm thick) of massive, planar laminated or hummocky cross-stratified sheets and lenses of siltstone, sandstone and sand-size dolostone (distal inner-shelf lagoon); (3) laminated dolostone that consists of very thin-bedded laminated or wave-rippled silt-size dolostone with

common intercalations of dolomitized oolitic and intraclastic grainstone layers, suggesting deposition close to fair weather wave base (proximal inner-shelf lagoon); (4) stromatolitic and thrombolitic dolostone (10–150 cm thick) containing isolated to laterally-linked columnar and domal stromatolite and/or thrombolite that show an upward decrease in relief (upper subtidal to lower intertidal); (5) stromatolites (up to 1–2 m thick) as planar tan- to buff-colored crinkly to wavy laminites overlain by gray to black planar or discrete to partially-linked microdigitate forms less than 1 cm wide and less than 10 cm high. This facies contains desiccation cracks, irregular to planar birdseyes, tepee structures, abundant halite casts and rare gypsum and/or anhydrite pseudomorphs (arid upper intertidal to supratidal).

The erosional surface at the base of asymmetric depositional cycles become more pronounced towards the shelf margin, suggesting prolonged exposure of the proximal 'shoal-complex'. The 'shoal complex' peritidal deposits overlie the back reef grainstone and stromatolite reef facies of the platform margin as a result of basinward progradation forming the highstand packages of long-term progradational sequences. Abundant halite casts and tepee structures and rare gypsum and anhydrite pseudomorphs in the shelf facies (Grotzinger 1985, 1986a, b) suggest that, contrary to Hoffman (1975), arid conditions prevailed during deposition of the Rocknest Formation.

21.7.2 Middle Cambrian Tidalites in Northern Iran

The Middle and Upper Cambrian was a time of extensive shallow marine carbonate ramp deposition in Iran. The ramp covered the length of the northern Alborz Mountains in northern Iran and the Persian Gulf in southwest Iran (Fig. 21.25) in the north-northeast facing Proto-Paleotethys passive margin of northern Gondwana (Y. Lasemi 2001), a width of several thousands of kilometers at the time of deposition. In the Alborz Mountains, the Middle- to Upper Cambrian deposits includes member 1 carbonates, member 2 mixed carbonate-siliciclastics and member 3 carbonates of the Mila Formation (Stocklin et al. 1964). In this summary, the tidal deposits of the lower part of member 2 in the Tuyeh section (location 1 in Fig. 21.25) of the eastern Alborz Mountains (Amin-Rasouli 1999) will be described. In the Tuyeh section, member 2 is 100 m thick and its lower part comprises two depositional sequences built mainly by peritidal facies. The lower sequence comprises lowstand, transgressive and highstand systems tracts built by meter-scale shallowing-upward cycles (Fig. 21.26).

The lowstand systems tract consists of interlayered light green- to redish brown, laminated argillaceous dolomudstone/dolomitic shale capped by reddish brown, fine- to very fine-grained lithic sandstone (Figs. 21.19a, b and 21.26a). The laminated shale-carbonate facies contain hopper halite casts (Fig. 21.19c) and has no subaerial exposure features. This facies association is interpreted as a coastal salina pond deposit. It resembles the carbonate-shale cycles described by Spencer and Demicco (1993) from the Middle Cambrian passive margin deposits of the Canadian Rocky Mountains. The brown lithic sandstone layers were probably deposited during the advance of siliciclastics into the coastal plain area during periods of continental flooding. The lower part of the transgressive systems tract consists of small-scale shallowing-upward cycles in which interlayered carbonate and siliciclastic facies just described above caps wavy- to planar stromatolite facies (Fig. 21.26b), which in turn change upward to planar- to wavy- to domal stromatolite capped by columnar stromatolite facies (Fig. 21.6e) recording the most transgressive facies. Columnar stromatolite bioherms are characterized by trapped peloids, ooids and intraclasts and absence of bioclasts recording deposition in a hypersaline and high energy subtidal lagoon to lower intertidal environments similar to Hamelin Pool in Shark Bay, Western Australia (e.g. Logan, et al. 1970). The highstand systems tract consists of meter-scale peritidal cycles. A typical and complete cycle that occurs in the lower part of the highstand tract (Fig. 21.26c) consists of (1) basal individual and compound columnar stromatolite bioherms subtidal lagoonal facies (Fig. 21.6e) grading upward into (2) laterally linked domal stromatolites lower intertidal facies (Fig. 21.9b, c), which in turn grades into (3) wavy to planar stromatolite upper intertidal facies containing desiccation cracks, planar fenestrae and calcite pseudomorphs after gypsum/anhydrite capped by (4) supratidal facies comprising fenestral and laminated dolomudstone with gypsum/anhydrite casts. The cycle is interpreted to have formed by progradation of an extensive tidal flat over a high energy lagoon covered

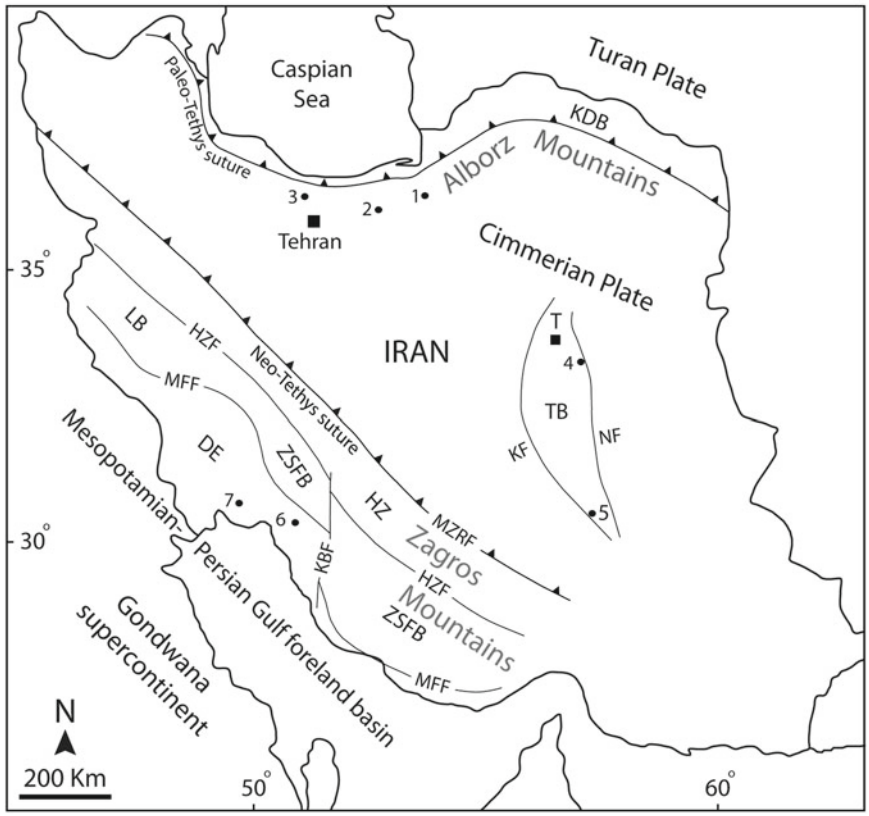

Fig. 21.25 Location map of Iran showing the structural features, plate boundaries and the basins/sub-basins mentioned in the text. The Cimmerian Plate between the Paleo-Tethys and Neo-Tethys sutures includes central Iran and the Alborz Mountains of northern Iran. The Zagros Mountains cover the area between the Neo-Tethys suture and Mountain Front Fault (*MFF*) in southwest Iran (fault traces are according to Berberian 1995 and Alavi et al. 1997). Numbered localities: (*1*) Tuyeh section; (*2*) Veresk section; (*3*) Elika section (*4*) Godare Sorkh section; (*5*) Eslamabad section; (*6*) Mish Mountain section; (*7*) Agha-Jari section. Abbreviations: *DE* Dezful Embayment, *HZ* High Zagros, *HZF* High Zagros Fault, *KBF* Kazrun-Borazjan Fault, *KDB* Kopet Dagh Basin, *KF* Kalmard/Kuhbanan Fault, *LB* Lurestan Sub-basin, *MZRF* Main Zagros Reverse Fault, *MFF* Mountain Front Fault, *NF* Nayband Fault, *T* Tabas (city), *TB* Tabas Basin, *ZSFB* Zagros Simply Folded Belt

with stromatolite reefs. Similar cycles are found in many other Cambrian successions (e.g. Demicco 1985; Spencer and Demicco 1993).

The overlying sequence (Fig. 21.26) includes transgressive and highstand systems tracts built mainly by small-scale shallowing-upward peritidal cycles consisting of (1) bioturbated bioclast/peloid wackestone-packstone (subtidal lagoon); (2) thin-bedded, interlayered dolomudstone and peloid bioclast grainstone (Fig. 21.12b, c) with ripple- wavy- lenticular bedding and vertical burrows (lower intertidal); (3) wavy to flat laminated stromatolite (upper intertidal); and (4) fenestral, mud-cracked dolomudstone with common lamination (disrupted in places forming collapse breccias) and calcite pseudomorphs after gypsum/anhydrite crystals or nodules (supratidal).

Tidal deposits of the Middle Cambrian member 2 of the Mila Formation were deposited in an arid homoclinal ramp, a vast epeiric sea that bordered the Proto-Paleotethys Ocean. Peritidal facies (predominantly tidal flat) constitute the bulk of the transgressive and highstand systems tracts and are arranged into high frequency 4th to 5th-order shallowing-upward cycles (Fig. 21.26b–f). They are interlayered with erosive-based fining-upward storm deposits consisting of intraclasts, peloids, ooids and bioclasts of mixed fauna, which suggest intermittent storm conditions during deposition (Y. Lasemi and Amin-Rasouli 2002).

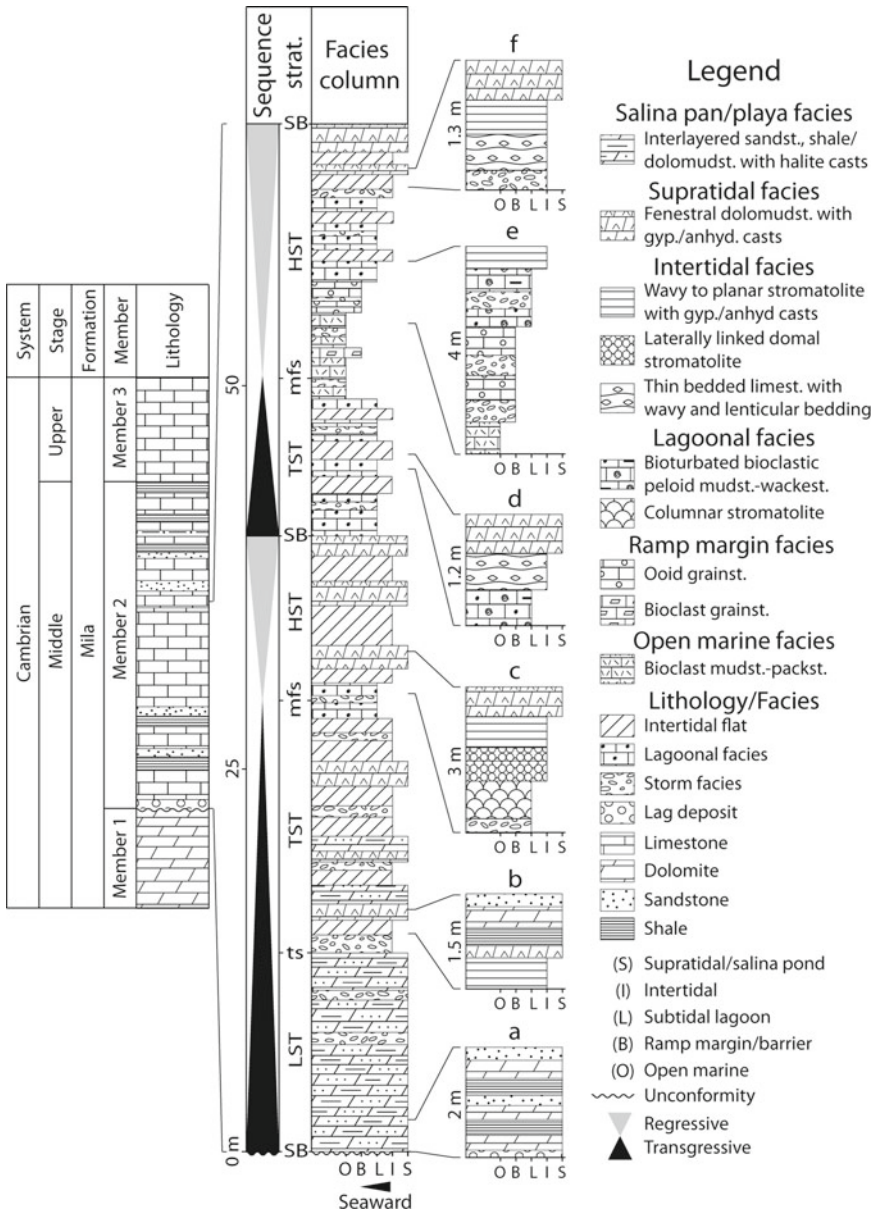

Fig. 21.26 Stratigraphic nomenclature and facies stratigraphy of the Middle Cambrian member 2 carbonates of the Mila Formation in the Tuyeh section (locality 1 in Fig. 21.25). Sequences (3rd-order cycles) are shown to the *left* of the facies column. Detail of a few small-scale shallowing-upward cycles is shown to the right. Note that the transgressive and highstand systems tracts of the lower sequence and the main part of the transgressive and highstand systems tracts of the upper sequence are composed of peritidal facies. These facies are arranged into small-scale shallowing-upward cycles composed of lagoonal- to intertidal- to supratidal or intertidal- to supratidal facies. Note also that the cycle stacking pattern is aggradational to progradational in the lowstand and highstand systems tracts; the pattern is aggradational to retrogradational in the transgressive packages. Black and gray triangles represent transgression and regression, respectively. Abbreviations: *HST* highstand systems tract, *LST* lowstand systems tract, *mfs* maximum flooding surface, *SB* sequence boundary, *ts* transgressive surface, *TST* transgressive systems tract

21.7.3 Tidalites of the Middle Ordovician St. Paul Group in Central Appalachians

The St. Paul Group (150–200 m thick) is a part of the Cambro-Ordovician platform carbonate succession in the central Appalachians, USA. In Maryland and Pennsylvania, the St. Paul succession consists mainly of lagoonal, tidal flat and freshwater coastal marsh facies (Mitchell 1985; Hardie 1986; Demicco and Hardie 1994) including: (1) thin-bedded interlayered LLH (Logan et al. 1964) stromatolite, unfossiliferous mudstone containing molds of cyanobacteria and intraclast packstone facies (coastal freshwater lake/supratidal marsh); (2) laminite facies (0.2–1 m thick) characterized by interlaminated planar- to wavy peloidal mudstone and crinkly stromatolite boundtone with birdseyes and desiccation cracks (supratidal levee); (3) bioturbated mudstone-wackestone facies (0.1–1.5 m thick) with low diversity fauna (mainly ostracods) and no internal layering (intertidal pond); (4) coarse peloidal sand- to pebble-sized micritic intraclast grainstone-packstone up to 0.3 m thick (meandering point bar deposit); (5) thick-bedded bioturbated lime mudstone facies with low to moderate diversity fauna (restricted to semi-restricted inner shelf lagoon to intertidal); (6) thick-bedded bioturbated wackestone/packstone and grainstones with diverse fauna including tabulate corals and bryozoans (open outer shelf lagoon).

In the St. Paul tidal deposits, bioturbated mudstone capped by mud cracked laminite facies dominate the lower part of tidal flat facies succession and are progressively replaced upward by thin-bedded and laminite facies that become more abundant upward near the boundary with the overlying coastal freshwater lake facies. According to Mitchell (1985), the closest modern analog of the St. Paul facies is the tidal flat system of the Bahamas including the Great Bahama Bank, Andros Island tidal flat and the inland freshwater marsh described by (Shinn 1983a, 1986). The absence of reefs and ooid grainstone, dominance of bioturbated peloidal mudstone, low diversity fauna, abundance of stromatolites and the absence of any trace of evaporites in the supratidal facies, all suggest the existence of a low energy, rainy tidal flat during the deposition of the St. Paul Group in central Appalachians (Mitchell 1985, Demicco and Hardie 1994).

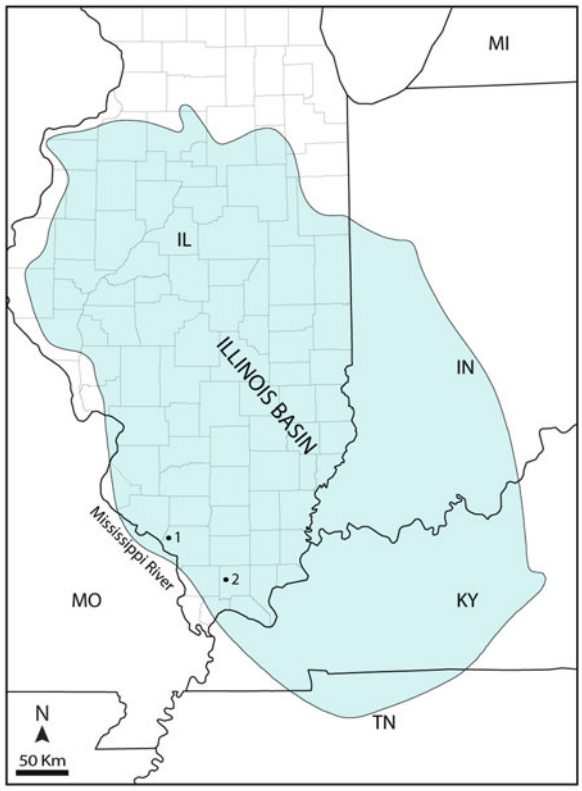

Fig. 21.27 Map of Illinois and neighboring states showing an outline of the Illinois Basin (From Buschbach and Kolata 1991) and the locations of sections used to prepare the composite section shown in Fig. 21.28. Numbered localities: (*1*) Kinkaid Creek section, Jackson County, Illinois; (*2*) Buncombe quarry section, Johnson County, Illinois

21.7.4 Mississippian Tidalites in the Illinois Basin

The intracratonic Illinois Basin (Kolata and Nelson 1991) covers parts of the states of Illinois, Indiana, Kentucky and Tennessee (Fig. 21.27) in the midcontinent of the United States (Buschbach and Kolata 1991). During the Mississippian (Early Carboniferous), several hundred meters of shallow marine carbonates were deposited on carbonate ramp platforms that opened into the deep Ouachita Trough to the south. Extensive peritidal facies have been described from the Cave Hill Member of the Upper Mississippian Kinkaid Formation (Y. Lasemi 1980, Y. Lasemi and Carozzi 1981). The Cave Hill Member (Swann 1963) is bounded by two limestone units namely the Negli

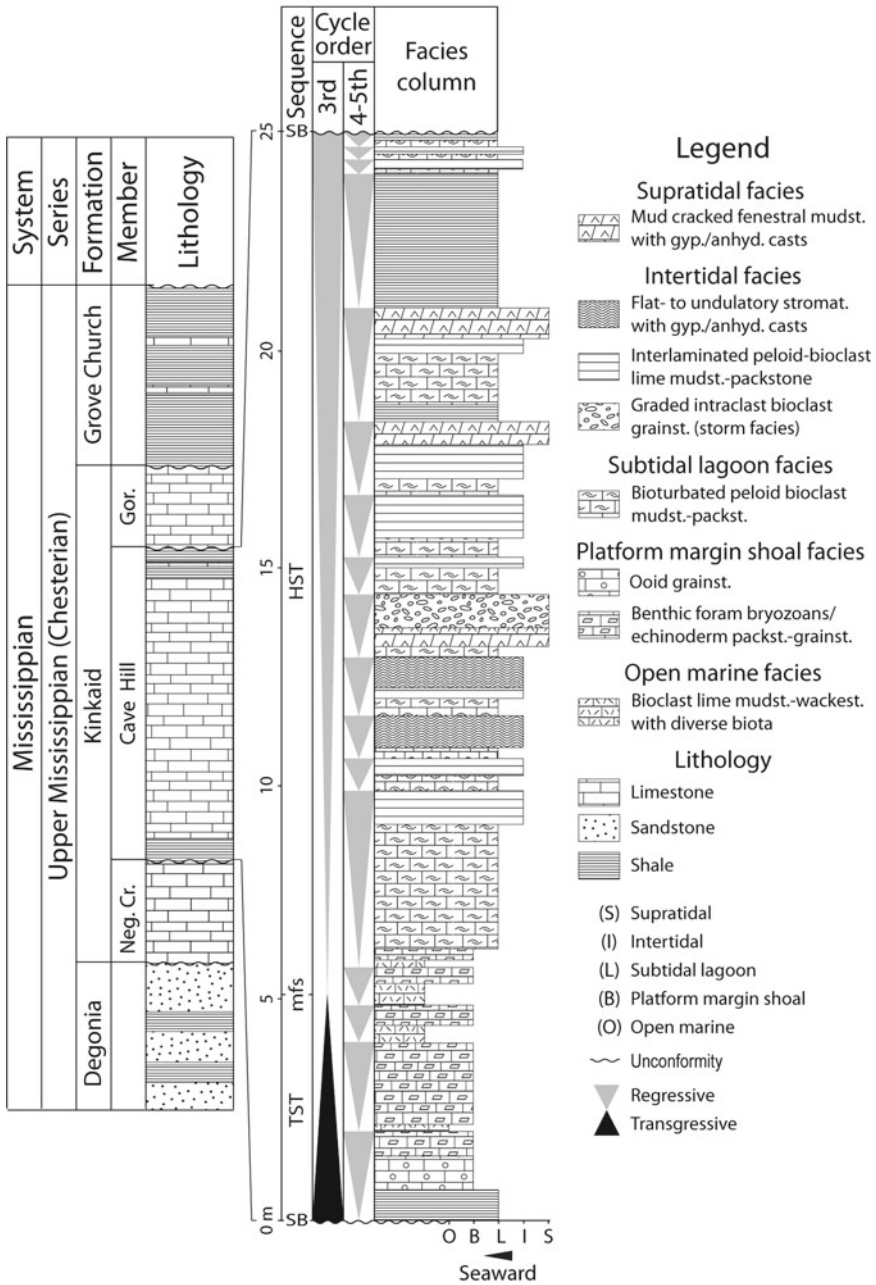

Fig. 21.28 Stratigraphic nomenclature and facies stratigraphy of the Cave Hill Member of the Kinkaid Formation in southwestern Illinois: The Cave Hill is an unconformity bounded sequence (3rd-order cycles) on which, several 4th to 5th-order shallowing-upward cycles are superimposed. The section is composed of the lower 6.5 m of the lower Cave Hill Member from locality 1 and the upper 18.5 m of the Cave Hill Member from locality 2 (see Fig. 21.27 for the location of sections). Note that small-scale peritidal cycles display progradational and aggradational stacking patterns and comprise the bulk of the highstand systems tract. *Black* and *gray triangles* represent transgression and regression, respectively. Abbreviations: *HST* highstand systems tract; *mfs* maximum flooding surface, *SB* sequence boundary, *TST* transgressive systems tract

Creek and the Goreville Members (Fig. 21.28). This summary concentrates on a composite section (Fig. 21.27, localities 1 and 2) of the Cave Hill Member in southwestern Illinois.

The Cave Hill Member mainly consists of cyclic peritidal deposits (Fig. 21.28) related to an arid and gently sloping homoclinal carbonate ramp similar to the modern Persian Gulf. Peritidal facies of the Cave

Hill include: (1) fenestral lime mudstone with calcite pseudomorphs after anhydrite and/or thickly interlaminated peloidal grainstone to mudstone with irregular to tabular fenestrae, root casts, and desiccation cracks (supratidal) (Figs. 21.15a, b, 21.17a and 21.18a, b); (2) millimeter-thick interlamination of micrite-rich and fine sand- to silt-sized bioclast/peloid-rich carbonates or flat- to wavy stromatolites commonly containing dolomudstone, molds of filamentous cyanobacteria, desiccation cracks and calcite pseudomorphs after lenticular gypsum (upper intertidal) (Figs. 21.3a, c, 21.9d, and 21.10c–e); and (3) bioturbated lime mudstone to packstone commonly containing peloids, oncoids and bioclasts (Fig. 21.5d) of a restricted fauna that commonly includes gastropods, ostracods, and benthic foraminifera (lower intertidal/subtidal lagoon). The Cave Hill Member represents an unconformity bounded depositional sequence (3rd-order cycle) on which are superimposed numerous small-scale fourth- to fifth-order cycles (Fig. 21.28). In the Cave Hill sequence, peritidal small-scale cycles comprise the bulk of the highstand systems tract and display aggradational and progradational stacking patterns (Fig. 21.28). The absence of peritidal deposits in the transgressive tract may be the consequence of a rather fast sea level rise during the onset of deposition of the Cave Hill Member.

A similar carbonate tidal deposit occurs in the lower part of the Middle Mississippian St. Louis Limestone of the Illinois Basin and its equivalent in the Michigan Basin. In southwestern Illinois, a peritidal succession with a basal unconformable boundary is present in the lower part of the lower St. Louis Limestone (Z. Lasemi and Norby 1999). This interval includes cyclic bioturbated lime mudstone to intraclast/bioclast peloid and/or oncoid wackestone-grainstone containing a low-diversity fauna (subtidal) capped by wavy- to planar stromatolites or laminated peloid mudstone-grainstone (lower intertidal) overlain by mud-cracked peloidal dolomudstone/lime mudstone (Fig. 21.17c) with fenestral fabric, calcite pseudomorphs after gypsum or dissolution collapse breccia (supratidal). The breccia beds change laterally to gypsum and anhydrite beds in the subsurface, thus, they are related to collapse of the overlying limestone layers after dissolution of gypsum and anhydrite beds (Saxby and Lamar 1957). The peritidal facies grades upward to deeper marine facies and is interpreted here as the lowstand systems tract of a depositional sequence. This interval is correlated with the lower part of the Bayport Formation in the Michigan Basin, which includes: (1) millimeter to centimeter thick beds of interlayered quartz sandstone and dolomudstone/lime mudstone with calcite pseudomorphs after gypsum, lamination, desiccation cracks, rain drop impressions, birdseyes, microbial lamination and heterolithic stratification including wavy, flaser and lenticular bedding (Figs. 21.11 and 21.12a) recording deposition in an arid tidal flat adjacent to an aeolian sand flat; (2) dark gray bioturbated ostracod mudstone and/or microbial laminites (Fig. 21.16a) interpreted as an intertidal pond facies; and (3) sandy peloid, restricted-fauna bioclast mudstone to packstone lagoonal facies (Y. Lasemi 1986). In the St. Louis and Bayport Formations, the peritidal deposits occur in the lower part of the sequence and are here interpreted to have been deposited during lowstand and transgressive sea level rise.

21.7.5 Triassic Tidalites of Northern and Central Iran

During the Triassic, thick shallow marine carbonates were deposited under arid conditions on carbonate ramps that covered the northern Cimmerian Plate of central and northern Iran (Paleo-Tethys margin) and the northeast Gondwanan continent (Neo-Tethys margin) of southwest Iran (Fig. 21.25). The Elika Formation (up to 1000 m thick) in northern Iran is the uppermost unit of a thick platform carbonate succession related to the north-facing Paleo-Tethys passive margin that existed from Devonian through early Late Triassic times (Y. Lasemi 2001). This summary discusses the lower and middle Elika (Lower-Middle Triassic) in the central Alborz Mountains of northern Iran (Paleotethys passive margin) and the Sorkh Shale Formation (the lower Elika equivalent) in the Tabas failed rift basin of east central Iran (Fig. 21.25).

21.7.5.1 Lower Elika Member

The unconformity bounded lower Elika is up to 200 m thick and consists of thin to thick-bedded limestone with thin shale intercalations. This summary concentrates on the lower Elika of the Veresk section and the middle Elika of the type locality (Fig. 21.25, localities 2 and 3, respectively) and is adopted from Jahani (2000). The lower Elika member consists of subtidal open marine and grainstone shoal facies in the lower part changing upward to lagoonal and intertidal facies (Fig. 21.29). Peritidal facies comprise the middle and

upper parts and include (1) heavily bioturbated gray bioclastic peloid lime mudstone-packstone with a restricted fauna (subtidal lagoon) (Figs. 21.3d, and 21.5a, b) that may be overlain by (2) an iron oxide-stained, 20–70 cm thick, bioclast (mainly small gastropods) grainstone (Fig. 21.13b) that may contain fenestral fabric and exposure features (beach ridge) and/or (3) very thin- to medium-bedded, laminated tan to light brown lime mudstone/dolomudstone with desiccation cracks (intertidal) or graded grainstone to lime mudstone containing bioclast/peloid and intraclast grains (intertidal channel). These facies are interlayered with numerous erosive-based, commonly graded intraclastic storm facies of various thicknesses (Fig. 21.4b–d) recording deposition under a storm dominated platform. Peritidal facies are arranged into 4th to 5th-order shallowing-upward cycles and comprise the main part of the highstand systems tract exhibiting progradational stacking pattern (Fig. 21.29).

In the northern Tabas failed rift basin (Fig. 21.25, locality 4), the lower Elika equivalent Sorkh Shale Formation consists almost entirely of tidal flat facies (Fig. 21.30) intercalated with numerous storm beds and comprise the transgressive and highstand systems tracts of a depositional sequence (Ghomashi 2008, Y. Lasemi et al. 2008). Southward, the carbonate-rich peritidal deposits grade into mixed-carbonate and quartz sandstone containing bimodal, spherical, and well-rounded sand grains with polished (frosted) surface, tabular bedding with internal laminations, herringbone cross-laminations/cross bedding, flaser and lenticular bedding. In the Eslamabad section (locality 5 in Fig. 21.25), sandstone beds are overlain and underlain, with sharp contacts, by shallowing-upward carbonate tidal flat cycles forming pure siliciclastic-pure carbonate double cycles (Fig. 21.19d). Sedimentary structures, super mature rounding and vertical association with carbonate tidal flat facies suggest deposition in tidal flat setting. The frosting and bimodal size distributions of the quartz grains suggest proximity to a desert environment (e.g. Klein 1977). The sand grains are interpreted as coming from aeolian dune sands which were transported over the carbonate tidal flat (at the time of emergence) and were subsequently reworked in the intertidal environment during the next platform flooding (Y. Lasemi et al. 2008).

21.7.5.2 Middle Elika Member

The middle member (up to 700 m thick) consists of very thin- to thick-bedded dolomite and dolomitic limestone and overlies the lower unit with a distinct interregional unconformity. In the type locality (Fig. 21.25), it is 200 m thick and consists almost exclusively of peritidal facies (Fig. 21.31) including: (1) laminated fenestral dolomudstone with desiccation cracks, tepee structures and calcite pseudomorphs after gypsum/anhydrite (supratidal facies) (Figs. 21.10a and 21.18c); (2) wavy to flat-laminated stromatolite with desiccation cracks (upper intertidal facies) (Fig. 21.6f). In some localities of the central Alborz Mountains, domal stromatolite/thrombolite bioherms related to upper subtidal/intertidal depositional settings have been recognized near the base of the member; (3) laminated peloid bioclast packstone to mudstone/dolomudstone with desiccation cracks that may display heterolithic stratification (lower intertidal facies); (4) fenestral bioclast peloid/intraclast grainstone (beach ridge facies); (5) erosive-based and laterally discontinuous layers of bioclast/peloid intraclast grainstone that grade upward to mudstone with tabular bedding and herringbone cross-bedding (intertidal channel facies) (Fig. 21.16b, c); and (6) gray peloid bioclast mudstone to packstone (lagoonal facies).

Tidal flat deposits constitute the bulk of the middle Elika and occur in the transgressive and highstand systems tract (Fig. 21.31). They are characterized by their light tan to cream color, thin to very thin bedding and common presence of micritic dolomite, desiccation cracks, tepee structures, laminations, birdseyes, gypsum/anhydrite casts/molds and collapse breccias. Short-term seaward progradation resulted in numerous shallowing-upward high frequency cycles that are superimposed on long-term third-order cycles (Fig. 21.31). In sharp contrast to lower Elika, the Middle Triassic middle Elika was deposited primarily under a fair weather condition.

21.7.6 Tidalites of the Upper Miocene Asmari Formation

The Upper Oligocene to Lower Miocene Asmari Formation (James and Wynd 1965) was deposited in the elongate Persian Gulf-Mesopotamian foreland

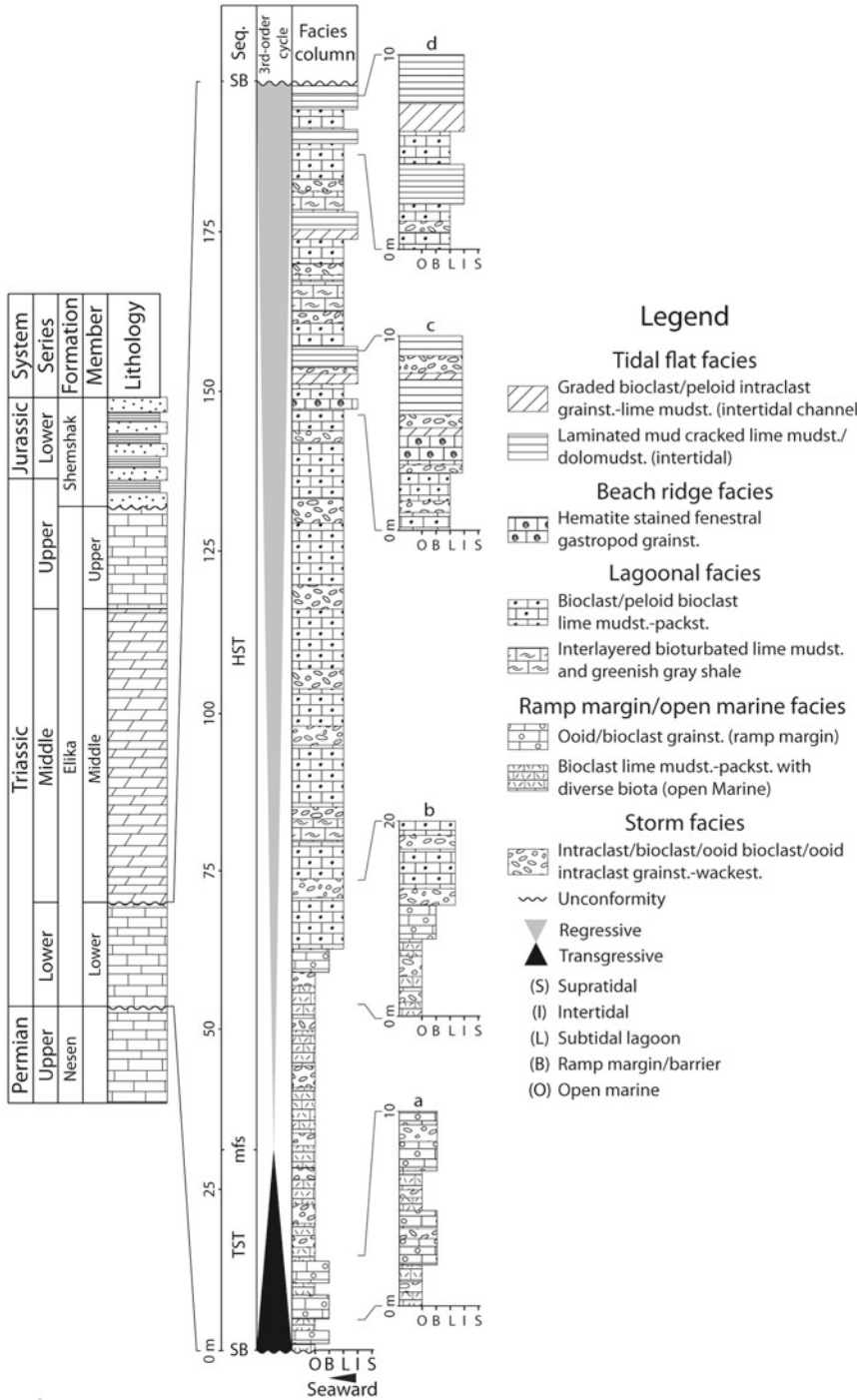

Fig. 21.29 Stratigraphic nomenclature and facies stratigraphy of the Lower Triassic lower member of the Elika Formation in the Veresk section of the Alborz Mountains (locality 2 in Fig. 21.25). Typical small-scale shallowing-upward cycles are shown to the right of facies column. Note that intertidal facies caps the small-scale cycles in the upper part of the highstand systems tract. Abundant storm facies (see the shallowing-upward cycles a through (**c**) indicate frequent storm conditions during the deposition of the lower Elika depositional sequence. Black and gray triangles represent transgression and regression, respectively. Abbreviations: *HST* highstand systems tract; *mfs* maximum flooding surface, *SB* sequence boundary, *TST* transgressive systems tract

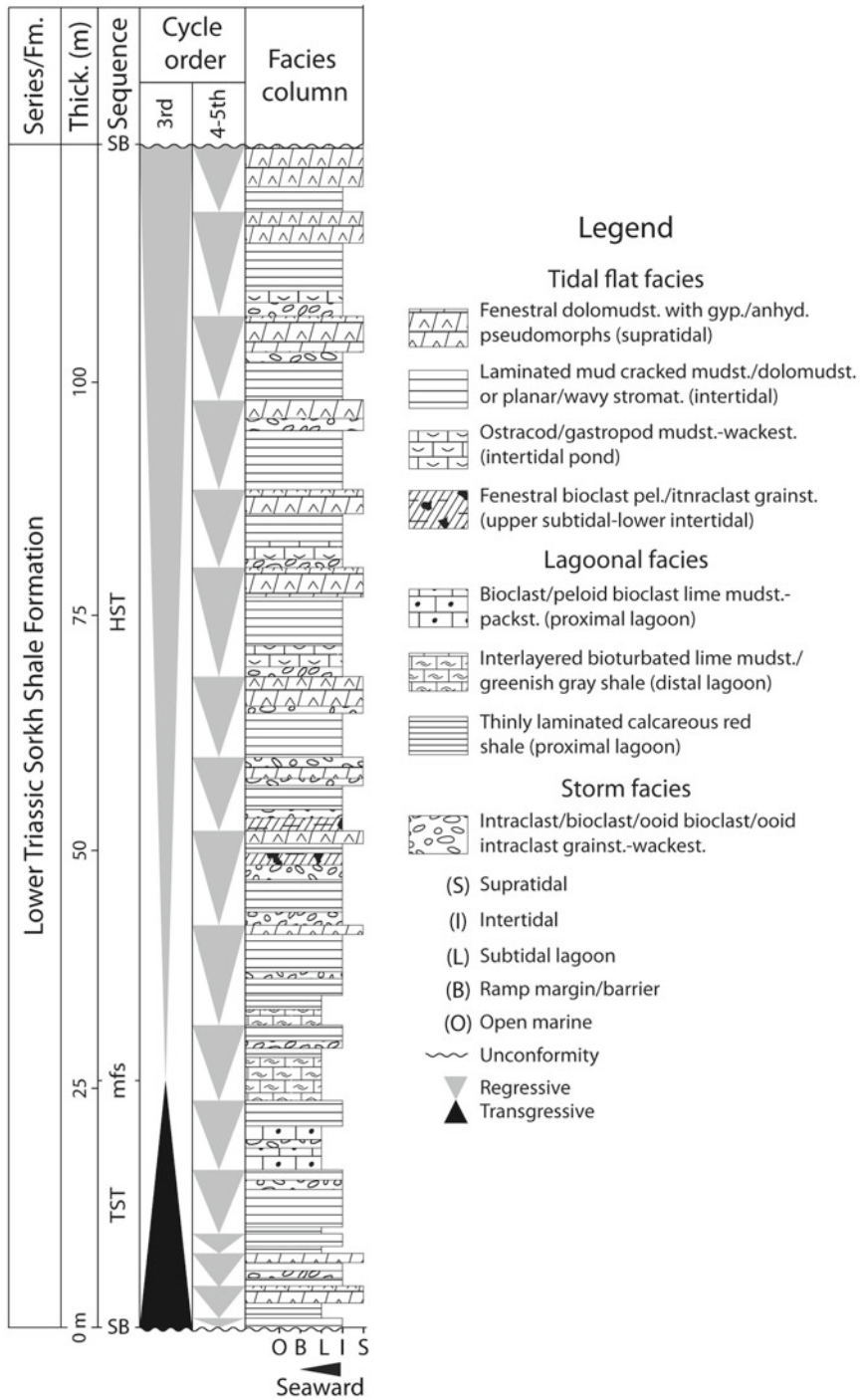

Fig. 21.30 Facies stratigraphy of the Sorkh Shale Formation in the Tabas rift basin, east central Iran (locality 4 in Fig. 21.25). Note that, except for the upper part of the transgressive systems tract, the sequence is entirely composed of tidal flat facies intercalated with storm deposits containing intraclasts, ooids and bioclasts derived from distal areas of the basin (not all storm layers are shown). Note also that the small-scale shallowing-upward cycle stacking pattern is retrogradational in the transgressive and progradational to aggradational in the highstand systems tracts, respectively (for comparison with the distally located Veresk section see Fig. 21.29). Black and gray triangles represent transgression and regression, respectively. Abbreviations: *HST* highstand systems tract, *mfs* maximum flooding surface, *SB* sequence boundary, *TST* transgressive systems tract

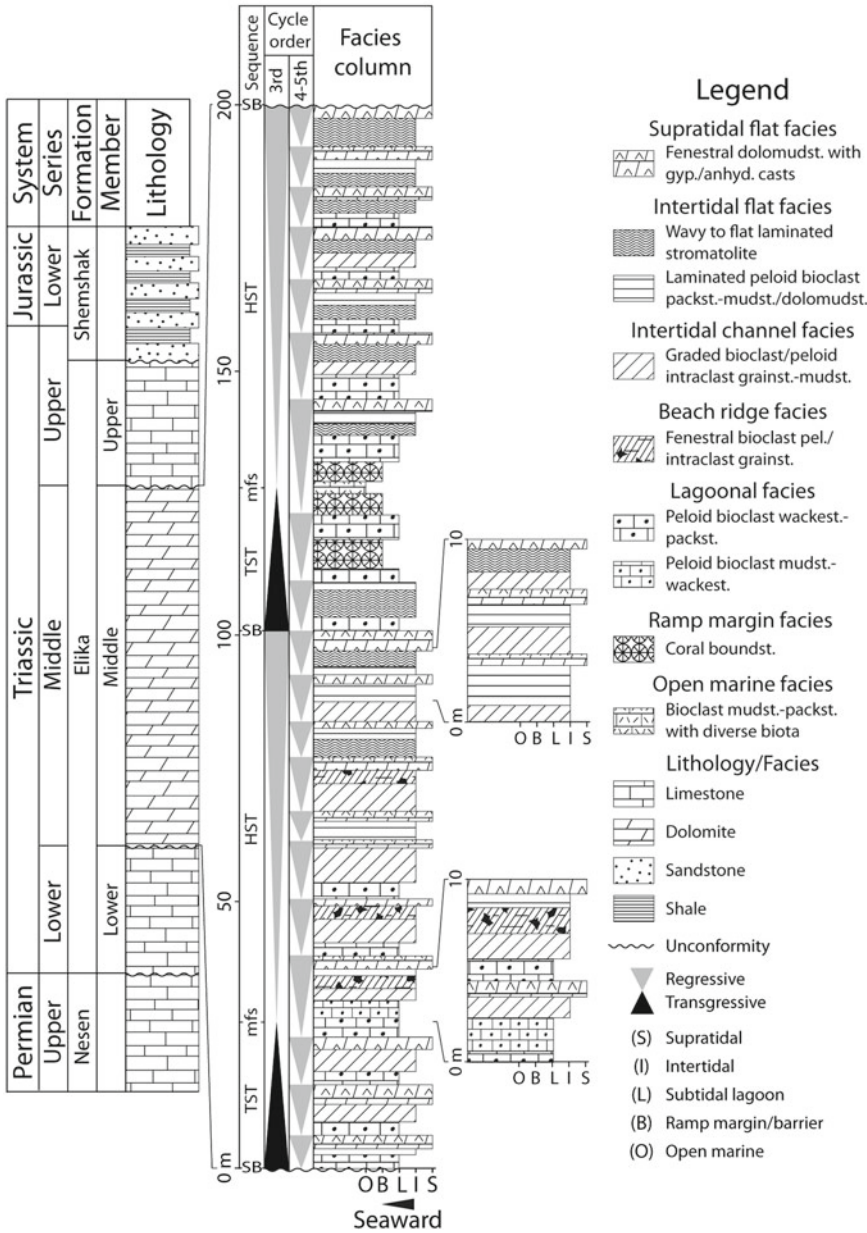

Fig. 21.31 Stratigraphic nomenclature and facies stratigraphy of the Middle Triassic middle Elika member in the type locality (locality 3 in Fig. 21.25). Note that the lower sequence and the highstand systems tract of the upper sequence are solely composed of peritidal facies that are arranged into small-scale shallowing-upward cycles composed of lagoonal- to intertidal- to supratidal or intertidal- to supratidal facies. Note also the progradational- to aggradational stacking pattern of the small scale cycles in the highstand systems tracts. Black and gray triangles represent transgression and regression, respectively. Abbreviations: HST highstand systems tract, *mfs* maximum flooding surface, *SB* sequence boundary, *TST* transgressive systems tract

basin in southwest Iran (Fig. 21.25). It is up to 500 m thick and consists mainly of shallow marine carbonates. This summary is adopted from Amin-Rasouli (2007) and describes the tidal deposits and sequences of the Lower Miocene upper member of the Asmari Formation in the Dezful Embayment, the Mish outcrop section and the Agha-Jari Well No. 61 (Fig. 21.25, localities 6 and 7, respectively).

The carbonate tidalites of the upper Asmari comprise (Fig. 21.32): (1) interlayered anhydrite and mud-

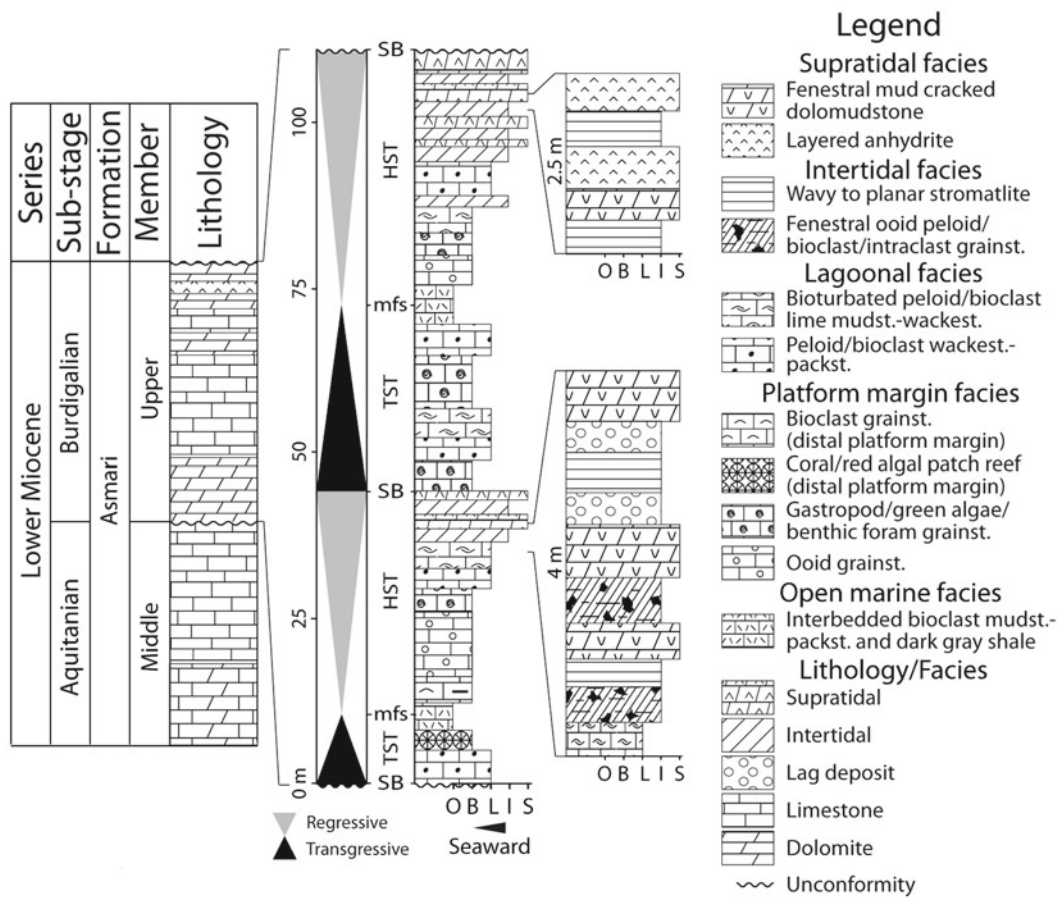

Fig. 21.32 Facies column and sequence stratigraphy of the Lower Miocene upper member of the Asmari Formation in southwest Iran (localities 6 and 7 in Fig. 21.25). The upper Asmari facies are arranged into numerous meter-scale shallowing-upward cycles superimposed on two depositional sequences consisting of transgressive and highstand systems tracts. Two typical small-scale shallowing-upward cycles are shown to the right of the facies column. Note that tidal flat deposits occur in the upper part of the highstand packages. Black and gray triangles represent transgression and regression, respectively. Abbreviations: *HST* highstand systems tract, *mfs* maximum flooding surface, *SB* sequence boundary, *TST* transgressive systems tract. Letters at the base of columns denote facies including: supratidal (*S*), intertidal (*I*), subtidal lagoon (*L*), ramp margin barrier/shoal (*B*), and open marine (*O*)

cracked dolomudstone containing fenestral fabric and/ or crystals/nodules or molds of gypsum/anhydrite (supratidal facies); (2) dolomitized wavy and flat-laminated stromatolite boundstone with desiccation cracks, birdseyes, small tepee structures and gypsum and/ or anhydrite crystals or pseudomorphs intercalated with erosive-based intraclast grainstone-packstone laminae (upper intertidal facies); (3) dolomitized fenestral ooid peloid/bioclast intraclast or fenestral bioclast grainstone with skeletal fragments of a restricted fauna (mainly miliolids) (beach ridge/lower intertidal facies); and (4) bioturbated peloid/bioclast lime mudstone to wackestone or packstone; bioclasts include ostracods, benthic foraminifera (mainly dentritinids and miliolids), gastropods and green algae (lagoonal facies) (Fig. 21.5c). These facies are arranged into meter-scale shallowing-upward cycles and display retrogradational and progradatiol stacking pattern in the transgressive and highstand systems tracts, respectively (Fig. 21.32). Tidal flat deposits are as much as 20 m thick and occur in the upper part of the highstand packages. Carbonate tidal sediments of the Asmari Formation were deposited in the ancestral Persian Gulf Foreland Basin in environments that are quite similar

to the southern portion of the present day arid Persian Gulf (e.g. Purser 1973).

A quite different tidal deposit of Late Miocene age (Messinian) has been reported from the Mediterranean Basin of southeast Spain (Riding et al. 1991). The Messinian carbonate tidalites are characterized by closely packed thrombolite and stromatolite domes forming a 12 m thick bioherm surrounded by ooids. Individual domes (up to 1.5 m high and 4 m across) are typically composite and consist of distinct juxtaposed stromatolite and thrombolite parts containing fine-medium grained ooid and peloid sand. Corals, red algae, vermitid gastropods and encrusting foraminifera are present in the stromatolite, suggesting a normal marine environment during deposition. Thrombolite is more abundant than stromatolite and consists of distinct clotted fabric and irregular fenestrae. These microbialites are closely comparable with modern "giant" subtidal columnar stromatolites observed at the Exuma chain of islands on the Bahamian platform (Dill 1991; Planavsky and Ginsburg 2009).

21.8 Concluding Remarks

The geological record of ancient carbonate peritidal deposits indicates deposition in the proximal areas of a tropical sea, particularly during global relative sea-level highstands, in carbonate platforms and environments that have recurred many times since the Early Proterozoic. As shown in the illustrative examples, ancient carbonate tidalites commonly consist of stacked high-frequency 4th- to 5th-order shallowing-upward cycles and may constitutes the bulk of the transgressive and highstand systems tract of a depositional sequence. The peritidal cycles in the geological record generally are characterized by evidence of a dry climate in the capping supratidal facies. Although supratidal marshes are widespread in the Bahamas and the neighboring modern humid platforms, ancient humid tidal flat and coastal marsh deposits like the Middle Ordovician St. Paul Group (see Sect. 21.7.3) are scarce. Rapid sea level fall and prolonged exposure of the tidal flat in a humid climate could lead to karstification and removal of the highstand packages of a depositional sequence, which commonly consists of peritidal cycle as in the existing Plio-Pleistocene record of the Bahamas. Comparison of the features of modern deposits with those in ancient carbonates suggests that sedimentary processes in carbonate platforms and environments have occurred repeatedly throughout geologic time.

References

Adams JE, Frenzel HN (1950) Capitan barrier reef, Texas and New Mexico. J Geol 58:289–312

Alavi M, Vaziri H, Seyed-Emami K, Lasemi Y (1997) The Triassic and associated rocks of the Nakhlak and Aghdarbad area in central and northeastern Iran as remnants of the southern Turanian active continental margin. Geol Soc Am Bull 109:1563–1575

Amin-Rasouli H (1999) Microfacies, depositional environments and sequence stratigrapohy of Shale and Top Quarzite units of the Lalum Formation and members 1 and 2 of the Mila Formation, Eastern Alborz (in Persian with English abstract), MS thesis, Tarbiat Moallem University, Tehran, Iran

Amin-Rasouli H (2007) Sequences stratigraphy of the Asmari Formation in Folded Zagros, Southwest Iran (in Persian with English abstract). Ph.D. thesis, Tarbiat Moallem University, Tehran, Iran

Bathurst RGC (1975) Carbonate sediments and their diagenesis. Elsevier, Amsterdam, 658 p

Beach DK, Ginsburg RN (1980) Facies succession of Pliocene-Pleistocene carbonates, northwestern Great Bahama Bank. Am Assoc Petrol Geol Bull 64:1634–1642

Berberian M (1995) Master "blind" thrust faults hidden under the Zagros folds: active basement tectonics and surface morphotectonics. Tectonophysics 241:193–224

Bosence D, Procter E, Aurell M, Kahla AB, Boudagher-Fadel M, Casaglia F, Cirilli S, Mehdie M, Nieto L, Rey J, Scherreiks R, Soussi M, Waltham D (2009) A dominant tectonic signal in high-frequency, peritidal carbonate cycles? A regional analysis of Liassic platforms from western Tethys. J Sed Res 79:389–415

Brown LF Jr, Fisher WL (1977) Seismic stratigraphic interpretation of depositional systems: examples from Brazilian rift and pull apart basins. In: Payton CE (ed) Seismic stratigraphy—applications to hydrocarbon exploration, American association ofpetroleum geological Memoir 26. American Association of Petroleum Geologists, Tulsa, pp 213–248

Burgess PM (2006) The signal and the noise: forward modelling of allocyclic and autocyclic processes influencing peritidal stacking patterns. J Sed Res 76:962–977

Burne RV, Moore LS (1987) Microbialites: organosedimentary deposits of benthic microbial communities. Palaios 2:241–254

Buschbach TC, Kolata DR (1991) Regional setting of Illinois Basin. In: Leighton MW, Kolata DR, Oltz DF, Eidel JJ (eds) Interior cratonic basins, American association petroleum geological Memoir 51. American Association Petroleum Geologists, Tulsa, pp 29–55

Carozzi AV (1989) Carbonate rock depositional models. A microfacies approach. Prentice Hall, Englewood Cliffs, 604 p

Catuneanu O (2006) Principles of sequence stratigraphy. Elsevier, Amsterdam, 375 p

Catuneanu O, Abreu V, Bhattacharya JP, Blum MD, Dalrymple RW, Eriksson PG, Fielding CR, Fisher WL, Galloway WE, Gibling MR, Giles KA, Holbrook JM, Jordan R, Kendall CGStC, Macurda B, Martinsen OJ, Miall AD, Neal JE, Nummedal D, Pomar L, Posamentier HW, Pratt BR, Sarg JF, Shanley KW, Steel RJ, Strasser A, Tucker ME, Winker C (2009) Towards the standardization of sequence stratigraphy. Earth Sci Rev 92:1–33

Cowan CA, James NP (1992) Diastasis cracks; mechanically generated synaeresis-like cracks in Upper Cambrian shallow water oolite and ribbon carbonates. Sedimentology 39:1101–1118

Dalrymple RW (1992) Tidal depositional systems. In: Walker RG, James NP (eds) Facies Models response to sea level change. Geological Association of Canada, St John's, pp 195–218

Davis RA (1983) Depositional systems. Prentice Hall, New Jersey, 669 p

De Benedictis D, Bosence DWJ, Waltham DA (2007) Tectonic control of peritidal carbonate parasequence formation: an investigation using forward tectono-stratigraphic modeling. Sedimentology 54:587–605

Demicco RV (1983) Wavy and lenticular bedded carbonate ribbon rocks of the Upper Cambrian Conococheague Limestone, Central Appalachians. J Sed Petrol 52:1121

Demicco RV (1985) Platform and off-platform carbonates of the Upper Cambrian of western Maryland, U.S.A. Sedimentology 32:1–22

Demicco RV, Hardie LA (1994) Sedimentary structures and early diagenetic features of shallow marine carbonates, Atlas Series 1, 265p

Dill RF (1991) Subtidal stromatolites, ooids, and crusted-lime muds at the Great Bahama Bank margin. In: Osborne RH (ed) From shoreline to abyss. SEPM Special Publication 46:147–171

Dupraz C, Reid RP, Braissant O, Decho AW, Norman RS, Visscher PT (2009) Processes of carbonate precipitation in modern microbial mats. Earth Sci Rev 96:141–162

Enos P, Perkins RD (1977) Quaternary sedimentation in South Florida, GSA Memoir 147. Geological Society of America, Boulder, 198 p

Flügel E (2010) Microfacies of carbonate rocks, analysis, interpretation and application. Springer, Berlin, 984 p

Ghomashi M (2008) Depositional environments and sequence stratigraphy of the Sorkh Shale and Shotori Formations (Lower-Middle Triassic) in the Tabas Block (in Persian with English abstract). Ph.D. thesis, Tarbiat Moallem University, Tehran, Iran

Ginsburg RN (1971) Landward movement of carbonate mud: new model for regressive cycles in carbonates (abstract): Am Assoc Petrol Geol Bull 55: 340

Ginsburg RN (1974) Introduction to comparative sedimentology of carbonates. Am Assoc Petrol Geol Bull 58:781–786

Ginsburg RN (1975) Tidal deposits, a casebook of recent examples and fossil counterparts. Springer, New York, 428 p

Goldhammer RK, Dunn PA, Hardie LA (1987) High frequency glacio-eustatic sea level oscillations with Milankovitch characteristics recorded in Middle Triassic platform carbonates in Northern Italy. Am J Sci 287:853–892

Goldhammer RK, Lehmann PJ, Dunn PA (1993) The origin of high-frequency platform carbonate cycles and third-order sequences (Lower Ordovician El Paso Gp, West Texas): constraints from outcrop data and stratigraphic modeling. J Sed Petrol 63:318–359

Grotzinger JP (1985) Evolution of early Proterozoic passive-margin carbonate platform, Rocknest Formation, Wopmay orogen, N. W. T., Canada. Ph.D. thesis, Virginia Polytechnic Institute, Blacksburg, Virginia, USA

Grotzinger JP (1986a) Evolution of early Proterozoic passive-margin carbonate platform, Rocknest Formation, Wopmay orogen, Northwest Territories, Canada. J Sed Petrol 56:831–847

Grotzinger JP (1986b) Cyclicity and paleoenvironmental dynamics, Rocknest platform, northwest Canada. Geol Soc Am Bull 97:1208–1231

Grotzinger JP (1989) Facies and evolution of Precambrian carbonate depositional systems: emergence of the modern platform archetype. In: Crevello PD, Wilson JL, Sarg JF, Read JF (eds) Controls on carbonate platform and basin development, SEPM Special Publication 44. SEPM, Tulsa, pp 79–106

Haq BU, Hardenbol J, Vail PR (1987) Chronology of fluctuating sea levels since the Triassic (250 million years ago to present). Science 235:1156–1166

Hardie LA (1977) Sedimentation on the modern carbonate tidal flats of northwest Andros Island, Bahamas, Johns Hopkins studies in geology 22. Johns Hopkins University Press, Baltimore, 202 p

Hardie LA (1986) Carbonate tidal-flat deposition: ten basic elements. Colo Sch Min Quart 81:3–6

Hardie LA (1987) Dolomitisation: a critical view of some current views. J Sed Petrol 57:166–183

Hardie LA, Shinn EA (1986) Carbonate depositional environments, modern and ancient. Part 3, Tidal flats. Colo Sch Min Quart 81, 74 p

Hardie LA, Bosellini A, Ginsburg RN (1986) Repeated subaerial exposure of subtidal carbonate platforms, Triassic, northern Italy: evidence for high frequency sea level oscillations on a 104 year scale. Paleoceanography 1:447–457

Hardie LA, Dunn PA, Goldhammer RK (1991) Field and modelling studies of Cambrian carbonate cycles, Virginia Appalachian—Discussion. J Sed Petrol 61:636–646

Hoffman P (1975) Shoaling-upward shale-to-dolomite cycles in the Rocknest Formation (Lower Proterozoic), Northwest Territories, Canada. In: Ginsburg RM (ed) Tidal deposits. Springer, Berlin, pp 257–265

Hoffman P (1976) Stromatolite morphogenesis in Shark Bay, Western Australia. In: Walter MR (ed) Stromatolites. Elsevier, Amsterdam, pp 261–271

Hunt D, Tucker ME (1992) Stranded parasequences and the forced regressive wedge systems tract: deposition during base-level fall. Sed Geol 81:1–9

Inden RF, Moore CH (1983) Beach environment. In: Scholle PA, Bebout DG, Moore CH (eds) Carbonate depositional environments, American association petroleum geologists memoir 33. American Association Petroleum Geologists, Tulsa, pp 211–265

Jahani D (2000) Sedimentary basin analysis of the Elika Formation in central and eastern Alborz (in Persian with English abstract). Ph.D. thesis, Islamic Azad University Science and Research Branch, Tehran, Iran

James NP (1984) Shallowing-upward sequences in carbonates. In: Walker KG (ed) Facies models, 2nd edn, Geoscience

Canada Reprint Series. Geological Association of Canada, Toronto, pp 213–228
James NP (1997) The cool-water carbonate depositional realm. In: James NP, Clarke JAD (eds) Cool-water Carbonates, SEPM Special Publication 56. SEPM (Society for Sedimentary Geology), Tulsa, pp 1–20
James GA, Wynd JG (1965) Stratigraphic nomenclature of Iranian oil consortium agreement area. Am Assoc Petrol Geol Bull 49:2182–2245
Kendall CGStC, Warren J (1987) A review of the origin and setting of tepees and their associated fabrics. Sedimentology 34:1007–1027
Kerans C, Tinker SW (1997) Sequence stratigraphy and characterization of carbonate reservoirs: SEPM short course notes 40, 130 p
Klein GdeV (1971) A sedimentary model for determining paleotidal range. Geol Soc Assoc Bull 82:2585–259
Klein GdeV (1977) Clastic tidal facies. Continuing Education Publishing Co, Champaign, 149 p
Klein GdeV (1998) Clastic tidalites__A partial retrospective view. In: Alexander CR, Davis RA, Henry VJ (eds) Tidalites: processes and products, SEPM Special Publication 61. SEPM (Society for Sedimentary Geology), Tulsa, pp 5–14
Koerschner WF, Read JF (1989) Field and modeling studies of Cambrian carbonate cycles, Virginia Appalachians. J Sed Petrol 59:654–687
Kolata DR, Nelson WJ (1991) Tectonic history of the Illinois Basin. In: Leighton MW, Kolata DR, Olts DF, Eidel JJ (eds) Interior cratonic Basins, American Association of Petroleum Geological Memoir 51. American Association Petroleum Geologists, Tulsa, pp 263–85
Lasemi Y (1980) Carbonate microfacies analysis and depositional environments of the Kinkaid Formation (Upper Mississippian) of the Illinois Basin. Ph.D. thesis, University of Illinois at Urbana-Champaign, Urbana, Illinois, USA
Lasemi Y (1986) Deepening-upward tidal-flat sequence within Bayport Formation, Upper Mississippian, Michigan Basin (abs) Am Assoc Petrol Geol Bull 70: 1068
Lasemi Y (1995) Platform Carbonates of the upper Jurassic Mozduran Formation in The Kopet Dagh Basin, NE Iran-facies, palaeoenvironments and sequences. Sed Geol 99: 151–164
Lasemi Y (2001) Facies analysis, depositional environments and sequence stratigraphy of the Upper Precambrian and Paleozoic rocks of Iran (in Persian). Geological Survey of Iran Publication, Tehran, 180 p
Lasemi Y, Amin-Rasouli H (2002) Microfacies and depositional environments of the storm deposits in the lower part of Member 2 of the Mila Formation in Tuyeh-Darvar area (in Persian with English abstract). Univ Tehran J Sci 28:33–52
Lasemi Y, Carozzi AV (1981) Carbonate microfacies and depositional environments of the Kinkaid Formation (Upper Mississsippian) of the Illinois Basin, U.S.A. In: Proceedings of 8th Congress Geol Argentino, San Luis. Actas 2:357–384
Lasemi Y, Ghomashi M, Amin-Rasouli H, Kheradmand A (2008) The Lower Triassic Sorkh Shale Formation of the Tabas Block, East Central Iran: succession of a failed-rift basin at the Paleo-Tethys margin. Carbonates and Evaporites 23:21–38
Lasemi Z, Norby RD (1999) Stratigraphy, paleoenvironments, and sequence stratigraphic implications of the Middle Mississippian carbonates in western Illinois. In: Lasemi Z, Norby RD, Devera JA, Fouke BW, Leetaru HE, Denny FB (eds) Middle Mississippian Carbonates and siliciclastics in Western Illinois, Illinois State Geological Survey Guidebook 31. Illinois State Geological Survey, Champaign, pp 1–18
Lasemi Z, Boardman MR, Sandberg PA (1989) Cement origin of supratidal dolomite, Andros Island, Bahamas. J Sed Petrol 59:249–257
Lehrmann DJ, Goldhammer RK (1999) Secular variations in parasequence and facies stacking patterns of platform carbonates a guide to application of stacking patterns analysis in strata of diverse ages and settings. In: Harris PM, Saller AH, Simo JA (eds) Advances in carbonate sequence stratigraphy: application to reservoirs, outcrops, and models, SEPM, Special Publication 63. SEPM, Tulsa, pp 187–225
Lehrmann DJ, Rankey EC (1999) Do meter-scale cycles exist? A statistical evaluation from vertical (1-D) and lateral (2-D) patterns in shallow-marine carbonate–siliciclastics of the "fall in" strata of the Capitan reef, Seven Rivers Formation, Slaughter Canyon, New Mexico. In: Saller AH, Harris PM, Kirkland BL, Mazzullo SJ (eds) Geological framework of the Capitan Reef, SEPM, Special Publication 65. SEPM (Society for Sedimentary Geology), Tulsa, pp 51–62
Logan BW, Rezak R, Ginsburg RN (1964) Classification and environmental significance of algal stromatolites. J Geol 72:68–83
Logan BW, Davies GR, Read JF, Cebulski DE (1970) Carbonate sedimentation and environments, Shark Bay, Western Australia. AAPG Mem 13:223p
Lokier S, Steuber T (2008) Large-scale intertidal polygonal features of the Abu Dhabi coastline. Sedimentology 56: 609–621
Miall AD (1997) The geology of stratigraphic sequences. Springer, Berlin, 433 p
Middleton GV (1973) Johannes Walther's law of correlation of facies. Geol Soc Am Bull 84:979–988
Mitchell RW (1985) Comparative sedimentology of shelf carbonates of the Middle Ordovician St. Paul Group, Central Appalachians. Sed Geol 43:1–41
Mitchum RM Jr, Vail PR, Thompson S III (1977) Seismic stratigraphy and global changes of sea-level, part 2: the depositional sequence as a basic unit for stratigraphic analysis. In: Payton CE (ed) Seismic stratigraphy—applications to hydrocarbon exploration, American Association of Petroleum Geologists Memoir 26. American Association Petroleum Geologists, Tulsa, pp 53–62
Planavsky N, Ginsburg RN (2009) Taphonomy of modern marine Bahamian microbialites. Palaios 24:5–17
Pomar L (2001) Types of carbonate platforms: a genetic approach. Basin Res 13:313–334
Posamentier HW, Allen GP (1999) Siliciclastic sequence stratigraphy: concepts and applications. SEPM Concepts in Sedimentology and Paleontology 7, 210 p
Pratt BR (1982) Stromatolite decline – a reconsideration. Geology 10:512–515
Pratt BR (2001) Calcification of cyanobacterial filaments: *Girvanella* and the origin of lower Paleozoic lime mud. Geology 29:763–766

Pratt BR (2002) Tepees in peritidal carbonates: origin via earthquake-induced deformation, with example from the Middle Cambrian of western Canada. Sed Geol 153:57–64

Pratt BR (2010) Peritidal carbonates. In: James NP, Dalrymple RG (eds) Facies models (3rd edn) Geological Association of Canada, St. John's, (in press)

Pratt BR, James NP (1982) Cryptalgal-metazoan bioherms of early Ordovician age in the St. Georges Group, western Newfoundland. Sedimentology 29:543–569

Pratt BR, James NP (1986) The St. George Group (Lower Ordovician) of western Newfoundland: tidal flat island model for carbonate sedimentation in shallow epeiric seas. Sedimentology 33:313–343

Pratt BR, James NP, Cowan CA (1992) Peritidal carbonates. In: Walker RG, James NP (eds) Facies Models response to sea level change. Geological Association of Canada Publication, St. Johns, pp 303–322

Preto N, Hinnov LA, DE Zanche V, Mietto P, Hardie LA (2004) The Milankovitch interpretation of the Latemar Platform cycles (Dolomies Itlay): implications for geochronology, biostratigraphy and Middle Triassic carbonate accumulation. In: D'Argenio B, Fischer AG, Silva IP, Weisert H, Ferreri V (eds) Cyclostratigraphy: approaches and case histories, SEPM, Special Publication 81. SEPM (Society for Sedimentary Geology), Tulsa, pp 167–182

Purser BH (1973) The Persian Gulf- Holocene carbonate sedimentation and diagenesis in a shallow epicontinental sea. Springer, New York, 471p

Purser BH, Evans G (1973) Regional sedimentation along the Trucial Coast, SE Persian Gulf. In: Purser BH (ed) The Persian Gulf- Holocene carbonate sedimentation and diagenesis in a shallow epicontinental sea. Springer, New York, pp 211–231

Rankey EC (2002) Spatial patterns of sediment accumulation on a Holocene carbonate tidal flat, Northwest Andros Island, Bahamas. J Sed Res 72:591–601

Read JF (1985) Carbonate platform facies models. Am Assoc Petrol Geol Bull 66:860–879

Reid RP, Visscher PT, Decho AW, Stolz JF, Bebout BM, Dupraz C, MacIntyre LG, Paerl HW, Pinckney JL, Prufert-Bebout L, Steppe TF, Des Marais DJ (2000) The role of microbes in accretion, lamination and early lithification of modern marine stromatolites. Nature 406:989–992

Reineck HE (1972) Tidal flats. In: Rigby JK, Hamblin WK (eds) Recognition of ancient sedimentary environments, SEPM Special Publication 16. Society of Economic Paleontologists and Mineralogists, Tulsa, pp 146–159

Reineck HE, Singh IB (1980) Depositional sedimentary environments, 2nd edn. Springer, New York, 551p

Riding R (1999) The term stromatolite: towards an essential definition. Lethaia 32:321–330

Riding R (2000) Microbial carbonates: the geological record of calcified bacterial–algal mats and biofilms. Sedimentology 47:179–214

Riding R, Braga JC, Martin JM (1991) Oolite stromatolites and thrombolites, Miocene, Spain: analogues of recent giant Bahamian examples. Sed Geol 71:121–127

Robbins LL, Blackwelder PL (1992) Biochemical and ultrastructural evidence for the origin of whitings: a biologically induced calcium carbonate precipitation mechanism. Geology 20:464–468

Saxby DB, Lamar JE (1957) Gypsum and anhydrite in Illinois: Illinois State Geological Survey Circular 226, 26p

Schlager W (2005) Carbonate Sedimentology and Sequence Stratigraphy. SEPM Concepts in Sedimentology and Paleontology *#8*, 200p

Scoffin TP, Stoddard DR (1983) Beachrock and intertidal cements. In: Goudie AS, Pye K (eds) Chemical sediments and geomorphology. Academic Press, London, pp 401–425

Shinn EA (1983a) Tidal flat environment. In: Scholle PA, Bebout D, Moore CH (eds) Carbonate depositional environments, American Association Petroleum Geologists Memoir 33. American Association Petroleum Geologists, Tulsa, pp 172–210

Shinn EA (1983b) Birdseyes, fenestrae, shrinkage pores and loferites: a re-evaluation. J Sed Petrol 53:619–628

Shinn EA (1986) Modern carbonate tidal flats: their diagnostic features. Colo Sch Min Quart 81:7–35

Shinn EA, Steinen RP, Lidz BH, Swart PK (1989) Whitings, a sedimentological dilemma. J Sed Petrol 59:147–161

Spence GH, Tucker ME (2007) A proposed integrated multi-signature model for peritidal cycles in carbonates. J Sed Res 77:797–808

Spencer RJ, Demicco RV (1993) Depositional environments of the Middle Cambrian Arctomys Formation, southern Canadian Rocky Mountains. Bull Can Petrol Geol 41:373–388

Stocklin J, Ruttner A, Nabavi M (1964) New data on the lower Paleozoic and Precambrian of north Iran. Geological Survey of Iran, report 1, 29 p

Strasser A, Pittet B, Hillgartner H, Pasquier JB (1999) Depositional sequences in shallow carbonate dominated sedimentary systems: concepts for a high-resolution analysis. Sed Geol 128:201–221

Swann DH (1963) Classification of the Genevievan and Chesterian (Late Mississippian) rocks of Illinois. Illinois State Geological Survey RI 216, 91 p

Tucker ME, Wright VP (1990) Carbonate sedimentology. Blackwell, Oxford, 482p

Van Wagoner JC, Posamentier HW, Mitchum RM, Vail PR, Sarg JF, Loutit TS, Hardenbol J (1988) An overview of the fundamentals of sequence stratigraphy and key definitions. In: Wilgus CK, Hastings BS, Kendall CG St C, Posamentier HW, Ross CA, Van Wagoner JC (eds) Sea-level changes, an integrated approach, SEPM Special Publication 42. Society of Economic Paleontologists, Mineralogists, Tulsa, pp 39–45

Van Wagoner JC, Mitchum RM Jr, Campion KM, Rahmanian VD (1990) Siliciclastic sequence stratigraphy in well logs, core, and outcrops: concepts for high-resolution correlation of time and facies, AAPG Methods in Exploration Series 7. American Association of Petroleum Geologists, Tulsa, 55 p

Wignall PH, Twitchett RJ (1999) Unusual intraclastic limestones in the Lower Triassic carbonates and their bearing on the aftermath of the end-Permian mass extinction. Sedimentology 46:303–316

Wilkinson BH, Diedrich NW, Drummond CN (1996) Facies succession in peritidal carbonate sequences. J Sed Res 66:1065–1078

Wilkinson BH, Drummond CN, Rothman ED, Diedrich NW (1997) Stratal order in peritidal carbonate sequences. J Sed Res 67:1068–1082

Wilkinson BH, Drummond CN, Diedrich NW, Rothman ED (1999) Poisson processes of carbonate accumulation on Paleozoic and Holocene platforms. J Sed Res 69:338–350

Wilson JL (1975) Carbonate acies in geologic history. Springer, Berlin, 471 p

Wright VP (1984) Peritidal carbonate facies models: a review. Geol J 19:309–325

Zecchin M (2010) Discussion – pomar Towards the standardization of sequence stratigraphy: is the parasequence concept to be redefined or abandoned? Earth Sci Rev 102:117–119